

17. ACCUMULATION RATES IN LEG 74 SEDIMENTS¹

N. J. Shackleton, The Godwin Laboratory, Free School Lane, Cambridge CB2 3RS, England
and
Members of the Shipboard Scientific Party²

ABSTRACT

Accumulation rates for the five sites drilled during Leg 74 of the *Glomar Challenger* are presented on a common timescale based on calibration of datum levels to paleomagnetic records in Leg 74 sediments for the Paleogene, and a new compilation by Berggren et al. (in press, a), for the Neogene, and using the seafloor-spreading magnetic anomaly timescale of Kent (in press). We present data on accumulation of total sediment, of foraminifers, of the noncarbonate portion, and of fish teeth that give a history of productivity, winnowing, carbonate dissolution, and nonbiogenic input to what was then a part of the South Atlantic at about 30°S.

INTRODUCTION

One of the purposes of drilling the Leg 74 sites was to examine the impact on sediment accumulation of those factors that vary with water depth: that is, winnowing and carbonate dissolution. It is hoped that the sediments recovered will provide a fruitful source of material for many studies in this topic in future years. In this chapter we explore some of the possibilities.

This chapter was written by NJS. It is particularly dependent on the nannofossil biostratigraphy of Hélène Manivit and Ming Jiang and on the palaeomagnetic data of Alan Chave; because of the constraints of time, distance, and language, responsibility for errors in the final compilation must be borne by NJS.

TIMESCALE

Oligocene to Recent

Any comparative study of sediment accumulation rates rests heavily on the estimation of the age of the sediment at specified points. Early in compiling the data it became apparent that a realistic conclusion to this study would require an even more major attack on biostratigraphy and magnetostratigraphy than we could achieve with only five sites; at the same time, any study of sediment accumulation rates that is based solely on literature estimates of the ages of biostratigraphic boundaries starts too far out of date to be valuable. A preliminary version of the new timescale of Berggren et al. (in press, a and b) became available in time for this study. In part, this timescale is dependent on Leg 74 data; its chief distinguishing feature is that it is calibrated to the seafloor-spreading magnetic anomaly timescale throughout (although it will, of course, be modi-

fied over the next few years as more sections become available). Table 1 shows datum levels used for Sites 525 to 529, together with the ages assigned to each. Unless otherwise specified, the age is that taken from the preliminary version of Berggren et al. (in press).

For the Pliocene and Pleistocene, we have in part used the timescale of Backman and Shackleton (1981), which is based on quantitative biostratigraphy in equatorial Pacific cores Vema (V) 28-179 and V28-185. However, because Backman has a different concept of the NN15-NN16 boundary (Backman and Shackleton, 1981) than that adopted by Jiang and Gartner (this volume), we have retained the latter's age of 3.1 Ma for this boundary.

Cretaceous to Eocene

For this part of the record we had access to sufficient palaeomagnetic and biostratigraphic data to calibrate a timescale directly (and to provide critical data for Berggren et al., in press). The magnetic inclination data are shown in Figure 1 as a function of depth below the sediment/water interface. Our procedure was first to plot all magnetic and biostratigraphic data on a common timescale, that of Hardenbol and Berggren (1978), by assigning a depth to each nannofossil datum and assigning to this depth an age determined from Hardenbol and Berggren. We did not use foraminiferal datums at the same time, because it is difficult to use datums from two different microfossil groups. The reason is, primarily, that for a single fossil group any biases introduced, for any reason, will emerge as different age estimates for each datum. With more than one group, it would become necessary to work with intervals defined by a different fossil group at each end; many of these intervals would be assigned zero duration on the Hardenbol and Berggren (1978) timescale because in that study many boundary ages were rounded to the nearest million years. We chose to work with the nannofossil data first because the majority of the datums had been significantly more closely located in depth than had the foraminiferal datums.

¹ Moore, T. C., Jr., Rabinowitz, P. D., et al., *Init. Repts. DSDP*, 74: Washington (U.S. Govt. Printing Office).

² These are: T. C. Moore, Jr., P. D. Rabinowitz (Leg 74 co-chief scientists); A. Boersma, P. E. Borella, A. D. Chave, G. Duée, D. Fütterer, M.-J. Jiang, K. Kleinert, A. Lever, H. Manivit, S. O'Connell, and S. H. Richardson.

Table 1. Age control points for Leg 74 sites.

Depth	Age (Ma)	Datum	Depth	Age (Ma)	Datum
Site 525					
0	0		172.93	55.66	Top Anomaly 24b
9.30	1.90	NN18-NN19	219.87	58.94	Middle Anomaly 25
18.26	3.10	NN15-NN16	237.91	60.75	Base Anomaly 26
32.60	3.60	NN12-NN13	258.75	63.03	Top Anomaly 27
47.82	4.50	NN12-NN13	260.77	63.54	Base Anomaly 27
57.00	5.00	Base <i>Ceratolithus acutus</i>	267.41	64.29	Top Anomaly 28
97.10	6.40	¹³ C "shift"	272.22	65.12	Base Anomaly 28
103.78	8.50	NN10-NN11	273.72	65.50	Top Anomaly 29
119.68	10.60	NN9-NN10	278.02	66.17	Base Anomaly 29
137.52	12.00	NN8-NN9	280.00	66.46	Cretaceous/Tertiary boundary
139.58	12.80	NN7-NN8	286.61	66.74	Top Anomaly 30
156.60	13.60	NN6-NN7	329.63	68.52	Base Anomaly 30
172.88	15.50	NN5-NN6			
193.15	17.00	NN4-NN5			
197.00	17.60	NN3-NN4			
207.95	18.00	NN2-NN3	12.84	1.45	Top <i>Cyclococcolithus maccintyrei</i>
226.75	22.80	NN1-NN2	19.70	1.90	NN18-NN19
256.65	23.70	NP25-NN1 (top <i>S. ciperoensis</i> and <i>Helicosphaera recta</i>)	27.85	3.10	NN15-NN16
278.60	25.30	NP24-NP25 (top <i>S. distentus</i>)	46.30	3.60	NN14-NN15
278.61	42.20	NP17-NP18 (base <i>Chiasmolithus oamaruensis</i>)	54.58	4.10	NN13-NN14
			55.60	4.50	NN12-NN13
			55.61	5.00	Base <i>C. acutus</i>
279.10	46.60	Top <i>C. gigas</i>	102.85	8.50	NN10-NN11
283.89	47.80	Base <i>C. gigas</i>	108.90	10.60	NN9-NN10
291.65	49.50	NP14-NP15 (base <i>Nannotettrina fulgens</i>)	115.34	12.00	NN8-NN9
310.55	52.60	NP13-NP14 (base <i>Discoaster sublodoensis</i>)	117.69	12.80	NN7-NN8
329.55	54.00	NP12-NP13 (top <i>Tribrachiatus orthostylus</i>)	118.50	13.60	NN6-NN7
336.55	54.50	NP11-NP12 (base <i>Discoaster lodoensis</i>)	118.51	16.50	NN5-NN6
349.00	55.50	NP10-NP11 (top <i>T. contortus</i>)	132.20	17.00	NN4-NN5
372.61	56.30	Base <i>T. orthostylus</i>	132.74	17.60	NN3-NN4
372.90	56.40	NP9-NP10 (base <i>Campylosphaera dela</i>)	145.21	18.00	NN2-NN3
387.84	56.80	Base <i>T. contortus</i>	149.11	20.45	Base Anomaly 6
391.55	57.60	Top <i>Fasciculithus</i> spp.	153.21	21.16	Base younger normal of Anomaly 6A
401.88	59.00	NP8-NP9 (base <i>D. multiradiatus</i>)	170.96	25.50	Top Anomaly 7
413.13	60.10	NP7-NP8 (base <i>Heliolithus riedeli</i>)	182.06	28.15	Top Anomaly 9
419.63	60.50	NP6-NP7 (base <i>D. mohleri</i>)	190.36	31.23	Top Anomaly 11
428.35	61.60	NP5-NP6 (base <i>H. kleinpellii</i>)	201.36	32.90	Base Anomaly 12
433.95	62.00	NP4-NP5 (base <i>F. tympaniformis</i>)	221.83	35.29	Top Anomaly 13
443.81	64.29	Top Anomaly 28	226.03	35.87	Base Anomaly 13
447.03	65.12	Base Anomaly 28	226.99	36.90	NP20-NP21 (top <i>D. barbadiensis</i> and <i>D. saipanensis</i>)
447.91	65.50	Top Anomaly 29			
450.99	66.17	Base Anomaly 29	238.13	40.20	NP17-NP18 (base <i>C. oamaruensis</i>)
451.71	66.44	Cretaceous/Tertiary boundary	248.59	46.17	Base Anomaly 20
456.69	66.74	Top Anomaly 30	253.50	47.80	Base <i>C. gigas</i>
475.15	68.42	Base Anomaly 30	257.05	48.75	Top Anomaly 21
476.50	68.52	Top Anomaly 31	258.24	50.34	Base Anomaly 21
489.26	69.40	Base Anomaly 31	261.40	52.29	Middle Anomaly 22
519.95	71.37	Top Anomaly 32	269.50	54.00	NP12-NP13 (top <i>T. orthostylus</i>)
			277.81	55.14	Top Anomaly 24
			284.80	55.40	NP11-NP12 (base <i>D. lodoensis</i>)
			306.86	56.30	Base <i>T. orthostylus</i>
			311.50	56.50	Base <i>D. diastypus</i>
			313.20	57.60	Top <i>Fasciculithus</i> spp.
			333.75	58.94	Middle Anomaly 25
			346.70	61.00	NP5-NP7
			379.70	62.00	NP4-NP5 (base <i>F. tympaniformis</i>)
			391.58	63.03	Top Anomaly 27
			395.20	64.90	NP2-NP3 (base <i>C. danicus</i>)
			398.60	65.30	NP2a-NP2b
			399.47	65.50	Top Anomaly 29
			405.97	66.17	Base Anomaly 29
			407.00	66.46	Cretaceous/Tertiary boundary
			413.34	66.74	Top Anomaly 30
			464.57	69.40	Base Anomaly 31
Site 526					
0	0		1.70	0.45	NN19-NN20
3.23	0.45	NN19-NN20	17.30	1.90	NN18-NN19
16.20	1.90	NN18-NN19	19.05	3.10	NN15-NN16
29.50	3.60	NN14-NN15	36.35	3.60	NN14-NN15
31.00	4.10	NN13-NN14	37.45	4.10	NN13-NN14
35.45	4.50	NN12-NN13	37.46	12.00	NN8-NN9
47.20	5.00	Base <i>C. acutus</i>	42.54	13.30	Mid NN7
67.87	8.50	NN10-NN11	55.25	15.50	NN5-NN6
80.08	10.60	NN9-NN10	56.43	17.00	NN4-NN5
89.73	12.00	NN8-NN9	69.73	17.60	NN3-NN4
94.21	12.80	NN7-NN8	74.05	18.00	NN2-NN3
106.75	13.60	NN6-NN7	82.05	22.80	NN1-NN1
114.63	15.50	NN5-NN6	118.55	23.60	NP25-NN1 (top <i>S. ciperoensis</i> and <i>H. recta</i>)
116.65	17.00	NN4-NN5			
117.45	17.60	NN3-NN4			
121.08	18.00	NN2-NN3			
122.00	22.80	NN1-NN2			
160.09	23.60	(top <i>S. ciperoensis</i> & <i>H. recta</i>)			
170.20	28.10	NP24-NP25 (top <i>S. distentus</i>)			
184.10	30.30	NP23-NP24 (base <i>S. ciperoensis</i>)			
209.60	34.60	NP22-NP23 (top <i>Reticulofenestra umbilica</i>)			
209.61	36.90	NP20-NP21 (top <i>D. barbadiensis</i> and <i>D. saipanensis</i>)			
226.20	37.80	NP18-NP19 (base <i>Isthmolithus recurvus</i>)			
Site 527					
0	0		1.70	0.45	NN19-NN20
14.00	1.90	NN18-NN19	17.30	1.90	NN18-NN19
18.97	2.40	NN16-NN17	19.05	3.10	NN15-NN16
23.42	3.10	NN15-NN16	36.35	3.60	NN14-NN15
48.15	4.10	NN13-NN14	37.45	4.10	NN13-NN14
59.10	5.00	Base <i>C. acutus</i>	37.46	12.00	NN8-NN9
104.12	8.50	NN10-NN11	42.54	13.30	Mid NN7
104.56	10.6	NN9-NN10	55.25	15.50	NN5-NN6
110.55	12.00	NN8-NN9	56.43	17.00	NN4-NN5
113.00	12.57	NN7-NN8	69.73	17.60	NN3-NN4
113.84	34.60	NP22-NP23 (top <i>R. umbilica</i>)	74.05	18.00	NN2-NN3
125.68	36.90	NP20-NP21 (top <i>D. barbadiensis</i> and <i>D. saipanensis</i>)	82.05	22.80	NN1-NN1
136.31	42.73	Base Anomaly 18	118.55	23.60	NP25-NN1 (top <i>S. ciperoensis</i> and <i>H. recta</i>)
137.61	44.66	Top Anomaly 20	138.15	28.10	NP24-NP25 (top <i>S. distentus</i>)
138.71	46.17	Base Anomaly 20	162.55	34.60	NP22-NP23 (top <i>R. umbilica</i>)
138.85	47.60	Top <i>Chiasmolithus gigas</i> (hiatus?)	186.07	35.10	NP21-NP22 (top <i>C. formosus</i>)
140.77	47.80	Base <i>C. gigas</i>	199.79	36.90	NP20-NP21 (top <i>D. barbadiensis</i> and <i>D. saipanensis</i>)
143.45	48.75	Top Anomaly 21	223.15	47.80	Base <i>C. gigas</i>
148.09	50.34	Base Anomaly 21	231.00	49.50	NP14-NP15 (base <i>N. fulgens</i>)
153.59	51.95	Top Anomaly 22	247.15	55.00	NP11-NP12 (base <i>D. lodoensis</i>)
154.73	52.62	Base Anomaly 22	264.50	56.30	NP9-NP10 (base <i>C. dela</i>)
163.88	54.70	Base Anomaly 23	273.25	59.00	NP8-NP9 (base <i>D. multiradiatus</i>)
			314.75	60.10	NP7-NP8 (base <i>D. riedeli</i>)
			319.80	60.50	NP6-NP7 (base <i>D. mohleri</i>)
			323.95	60.75	Base Anomaly 26
			331.90	61.60	NP5-NP6 (base <i>H. kleinpellii</i>)
			348.70	62.00	NP4-NP5 (base <i>F. tympaniformis</i>)
			372.80	64.90	NP2-NP3 (base <i>C. danicus</i>)
			383.63	65.90	NP1-NP2 (base <i>C. tenuis</i>)
			385.10	66.17	Base Anomaly 29
			387.77	66.46	Cretaceous/Tertiary boundary
			394.17	66.74?	Top Anomaly 30 (hiatus)

Note: The species used on this leg to define Paleogene zone boundaries are explicitly stated as they are not invariably those originally used by Martini (1971).

After these preliminary plots were made, it was easy to recognize many of the magnetic anomalies. The next step was to make adjustments to the timescale so as to bring the magnetic pattern into alignment with our chosen seafloor-spreading timescale, that of Kent (in press). Although earlier work by Chave (this volume) was based on the timescale in the elegant presentation of Ness et al. (1980), we became convinced that Kent (in press) had made significant improvements to the accuracy of the seafloor magnetic anomaly timescale. Several iterations were necessary before a consistent picture was obtained.

Table 2 gives the ages of nannofossil datums as estimated in each of Sites 525, 527, and 528 on the basis of interpolation between magnetostratigraphic horizons. For each of these datums, the figure finally adopted is also given.

There are several types of error involved in these estimates. First, we may have misidentified the reversals observed in the sediment. It is hoped that this does not apply to any reversal, but there are three regions of significant uncertainty. Around Anomalies 23 and 24, we encountered considerable difficulty in reaching a definite solution, and the problem was exacerbated by the obvious changes in sedimentation rate around that time. Second, none of the sites recovered a good fossiliferous late Eocene section, so that the timescale is poorly constrained in that region. Third, although the data from Site 528 contain several large gaps during the Oligocene, we believe that the majority of the horizons are correctly identified; however, the identification of Anomaly 6 in the Miocene may be incorrect. We have not taken account of the estimates based on this identification. It should be remarked, however, that the accumulation rate data for Site 528 have been compiled using these magnetic data and show a very smooth plot of both carbonate and noncarbonate accumulation. It is likely that the large excursions in accumulation rate in the other sites at about 22 Ma are an artifact resulting from an error in this part of the timescale; it is thus also likely that our age for the NN1/NN2 boundary is inappropriate.³

In general, magnetic reversals are located in the core to within about 10 cm, but the true uncertainty in the depth at which the reversal was present in the undisturbed sediment may be several meters in situations where recovery was poor. A good example is the Eocene/Oligocene boundary at Site 528. The boundary is close to the top of Core 528-13 and is nominally only 96 cm below the base of Anomaly 13, which is within Core 528-12. However, recovery in Core 13 was only about 3 m, so that the true position of the boundary may have been several meters below Anomaly 13. In this case, the age estimated would have been consistent with that given by Berggren et al. (in press, b), which in turn is based on Italian sections (Lowrie et al., 1982) and on

Table 2. Ages of nannofossil datum levels for Leg 74, estimated by interpolation between magnetic datums.

Datum	Depth in Hole (m)	Age derived from Depth in this Site	Age Used (estimate based on data from all sites)
Site 525			
Base <i>Cruciplacolithus tenuis</i>	449.30	65.80	65.90
Base <i>C. primus</i>	451.00	66.17	66.10
Cretaceous/Tertiary*	451.71	66.33 (down)	66.46
Cretaceous/Tertiary*	451.71	66.29 (up)	66.46
Base <i>Micula murus</i>	465.76	67.57	67.5
Base <i>Lithraphidites quadratus</i>	483.50	69.00	69.0
Top <i>Quadrum trifidum</i>	521.50	71.47	71.5
Site 527			
Base <i>Nannotetra fulgens</i>	146.02	49.56	49.5
Base <i>Discoaster sublodoensis</i>	152.74	51.68	51.7
Top <i>Tribrachiatus orthostylus</i>	160.34	53.90	54.0
Base <i>D. lodoensis</i>	170.50	55.40	55.4
Base <i>T. orthostylus</i>	182.34	56.32	56.3
Top <i>T. contortus</i>	182.34	56.32	56.3
Base <i>Campylophaera dela</i>	182.34	56.32	56.4
Base <i>D. diastypus</i>	189.00	56.78	56.5
Base <i>T. contortus</i>	189.00	56.78	56.8
Top <i>Fasciclitus</i> spp.	201.05	57.63	57.6
Top <i>Ericsonia robusta</i>	213.80	58.52	58.6
Base <i>D. multiradiatus</i>	220.75	59.03	59.0
Base <i>Heliolithus riedeli</i>	231.96	60.15	60.1
Base <i>D. mohleri</i>	235.08	60.47	60.5
Base <i>H. kleinpellii</i>	245.43	61.57	61.6
Base <i>F. tympaniformis</i>	249.78	62.05	62.0
Base <i>Ellipsolithus macellus</i>	258.03	62.95	63.0
Base <i>Chiasmolithus danicus</i>	271.10	64.93	64.9
Base NP2B	272.85	65.28	65.25
Base <i>Cruciplacolithus tenuis</i>	276.19	65.89	65.9
Base <i>C. primus</i>	277.75	66.13	66.10
Cretaceous/Tertiary*	280.00	66.47 (down)	66.46
Cretaceous/Tertiary*	280.00	66.48 (up)	66.46
Base <i>M. murus</i>	303.50	67.44	67.5
Site 528			
Base NN2	146.70	20.03	22.80
Top <i>Sphenolithus ciperoensis</i>	169.60	25.60	23.6
Top <i>Helicosphaera recta</i>	169.60	25.60	23.6
Top <i>S. distentus</i>	179.20	28.20	28.1
Base <i>S. ciperoensis</i>	187.90	30.56	30.3
Top <i>R. umbilica</i>	203.60	33.16	34.6
Top <i>Cyclococcolithus formosus</i>	215.20	34.52	35.1
Top <i>D. barbadensis</i>	226.90	36.14	36.9
Top <i>D. saipanensis</i>	226.90	36.14	36.9
Base <i>Nannotetra fulgens</i>	257.60	49.49	49.5
Top <i>T. orthostylus</i>	269.50	53.95	54.0
Base <i>D. lodoensis</i>	284.80	54.82	55.4
Top <i>T. contortus</i>	303.00	55.87	56.3
Base <i>T. orthostylus</i>	306.80	56.08	56.3
Base <i>C. dela</i>	311.50	56.50	56.4
Base <i>D. diastypus</i>	311.50	56.50	56.5
Top <i>Fasciclitus</i> spp.	313.20	57.60	57.6
Top <i>E. robusta</i>	329.10	58.64	58.6
Base <i>D. multiradiatus</i>	334.10	58.97	59.0
Base <i>D. mohleri</i>	346.70	59.87	60.5
Base <i>H. kleinpellii</i>	346.70	59.87	61.6
Base <i>F. tympaniformis</i>	379.70	62.24	62.0
Base <i>E. macellus</i>	390.50	63.01	63.0
Base <i>C. danicus</i>	395.20	64.20	64.9
Base NP2b	398.60	65.23	65.25
Base <i>C. tenuis</i>	404.20	65.99	65.90
Base <i>C. primus</i>	405.00	66.07	66.10
Cretaceous/Tertiary*		66.28 (down)	66.46
Cretaceous/Tertiary*		66.41 (up)	66.46

Note: * = Shipboard determination of the boundary. See Manivit (this volume) for detailed discussion.

DSDP Site 522 (Poore et al., in press; Tauxe et al., in press).

In most cases these problems are more important sources of uncertainty than of error in locating the nannofossil horizons, which have mostly been positioned to within one or two meters in the cores (although, again, the true uncertainty in the position of the datum in the

³ After this work was completed, NJS became aware that there were difficulties in recognizing *Discoaster druggi*, the marker for the NN1/NN2 boundary, in Leg 74 sites (Jiang and Gartner, this vol.). This probably accounts for the difficulty we encountered in reconciling the positions of the boundary in the sites with the age assigned by Berggren et al. (in press, a).

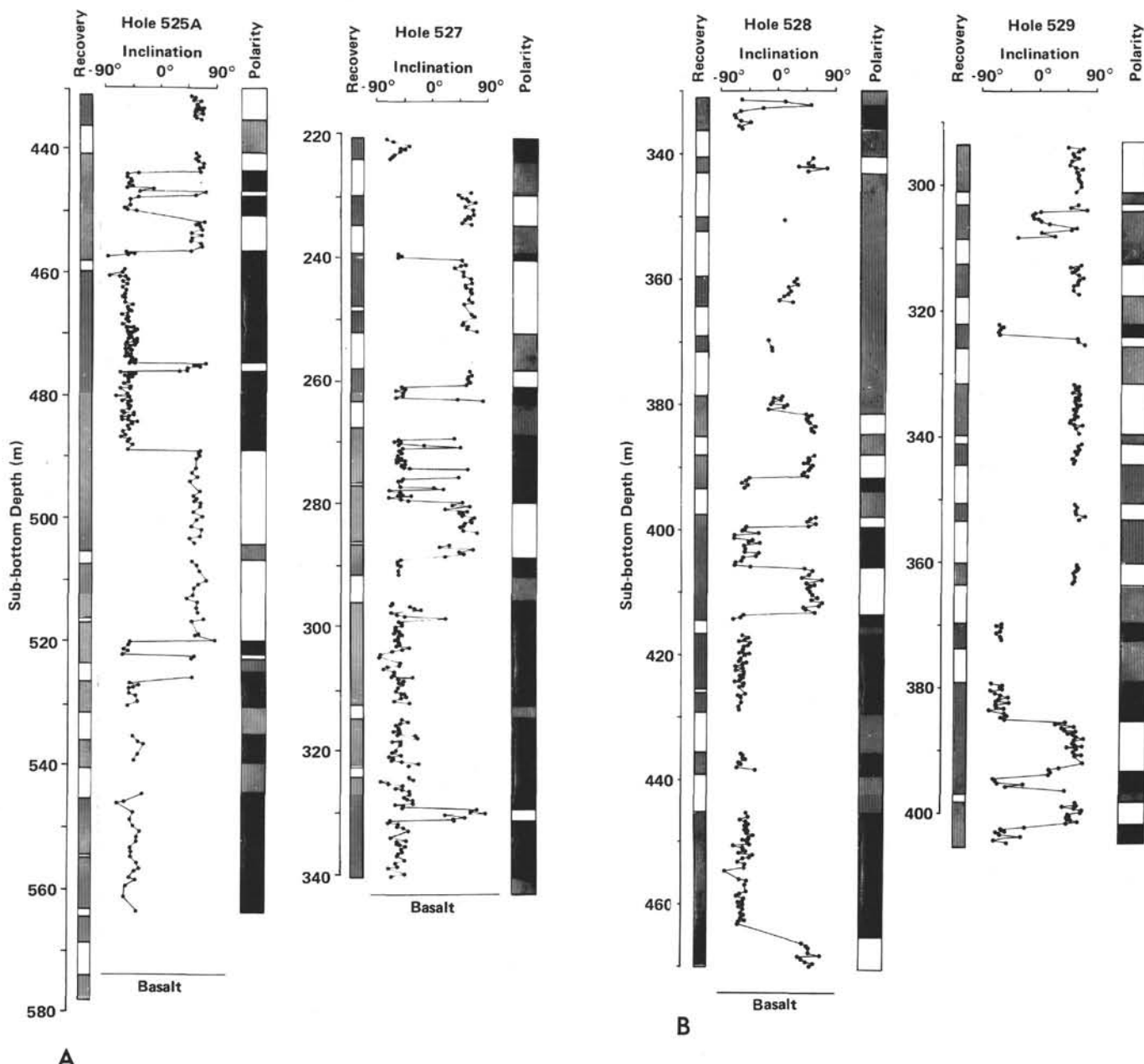


Figure 1. Magnetic inclination data plotted as a function of depth in hole. A. Hole 525A and lower part of Hole 527. B. Lower part of Hole 528 and Hole 529. C. Upper parts of Holes 527 and 528. The raw data for these figures are available from DSDP. For details of measurements, see Chave (this volume). (Black, normal; white, reversed; lines, no data [disturbed or unrecovered] or not interpreted [low inclination].)

sediment is always greater than the uncertainty in its location within a core).

Despite the range of preservational states, we consider that the nannofossil datums used are probably applied rather consistently among sites. However, there may well be inconsistencies in relation to other workers and other regions, and these may affect the applicability to our work of age estimates given by Berggren et al. (in press, a and b).

Finally, all datums that do not coincide with magnetic reversals (and any datum which appears to coincide with a reversal should be regarded with scepticism because of the risk that the two are brought together at a hiatus) have to be dated on the assumption of uniform

sediment accumulation between two magnetic reversals. Dating of events in the long reversed interval between Anomalies 24 and 25 must be regarded as speculative at present, since accumulation rates were clearly changing rapidly during this interesting interval.

The Cretaceous/Tertiary boundary has been the subject of detailed studies (Manivit, this volume). We have made an attempt to estimate the age of this horizon as precisely as possible. It is clear that at all sites there is a major sedimentation change at this boundary, so that we have made independent estimates of its age by extrapolating upward, using boundaries of Anomaly 30 and below, and downward, using Anomaly 29. For consistency, we have used the shipboard position of the

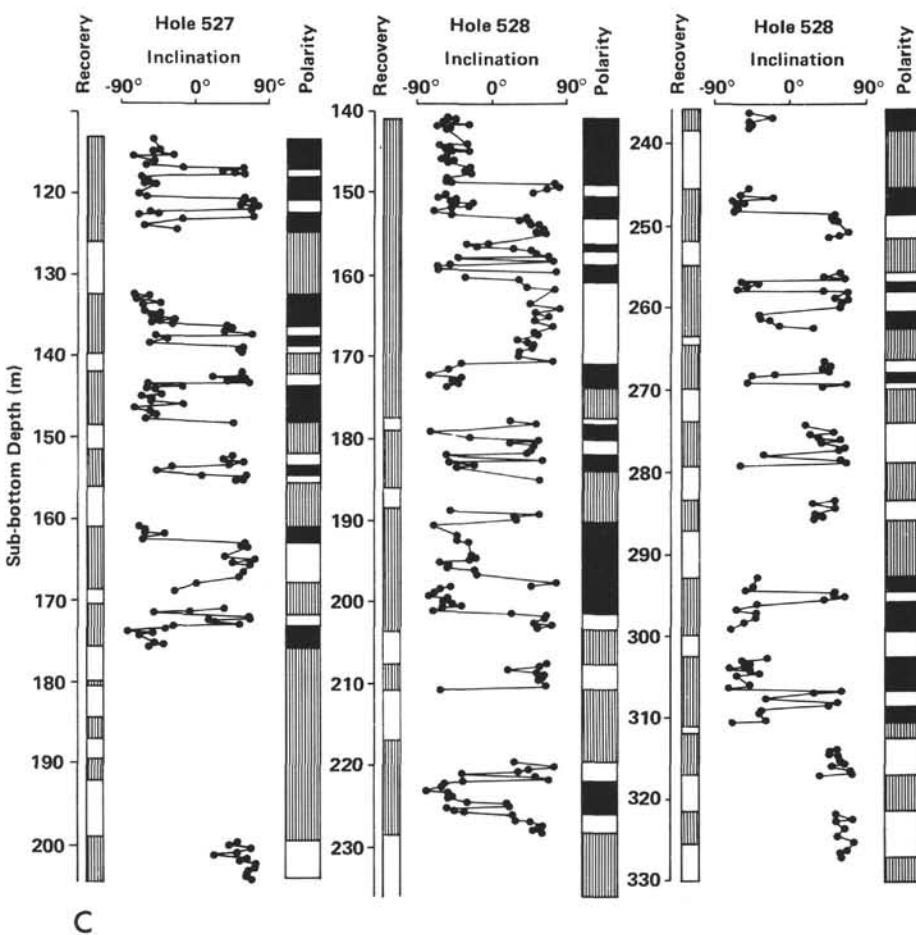


Figure 1. (Continued).

"sedimentological boundary" rather than involving ourselves in the finest points of biostratigraphy. It will be seen from Table 2 that the estimates for the boundary vary from ~66.3 to ~66.5 Ma. We have adopted a value of 66.46 Ma, the mean of two estimates from Site 527 and one from Site 528. We show later that Site 525 experienced considerable winnowing, which may reduce the reliability of its estimates; moreover, the lowermost Danian at that site is represented by about 1 m of drilling breccia. In Hole 528, the lowermost Danian shows rather irregular sedimentation and is regarded as less trustworthy. The accumulation rate data for noncarbonate sediments actually show a slight rise in the interval between 67 and 66.46 Ma when we use this figure. This rise is probably an artifact, but experiments with a slightly younger age generated other anomalous results and we believe that 66.46 Ma is the best figure that can be derived from the present data. It is very important for future studies around this boundary that seafloor-spreading timescales do not introduce a change in the spreading rate at this time and, furthermore, that as modifications are made (as they surely will be), a clear perspective is kept on the relationship between the boundary and the magnetic reversals.

Figure 2 shows the inferred positions of normal and reversed sedimentary sections for each site. The first point that should be made is that the position of Anom-

alies 27 to 30 is quite unambiguous (Chave, this volume). Equally, the calibration to these anomalies of the biostratigraphic datums agrees well with previous work in the Gubbio section (Lowrie and Alvarez, 1977; Roggenthen and Napoleone, 1977). A consistent position for Anomaly 26 is found in Sites 527 and 529, and one for Anomaly 25 in Sites 527 and 528. The thickness of sediment representing Anomaly 26 is rather small; for Anomaly 25 it is good.

When we come to Anomaly 24 the situation is less clear. According to the interpretation we have adopted, Sites 527 and 528 both preserve parts of Anomalies 23 and 24. The internal consistency between the two sites is acceptable, but changes in sedimentation rate are required. On the other hand, since both seafloor-spreading rates and true accumulation rates were varying around that time, it will be a few years before we have a clear understanding of this interval.

A key to the correct interpretation of the middle Eocene sequence is the identification of Anomaly 21 in Core 527-17. On Leg 73, Site 523 was drilled on Anomaly 21 as determined by seafloor magnetic data, and drilling was terminated above the base of the section in a reversed interval which is very reasonably interpreted as that between Anomalies 20 and 21 (Tauxe et al., in press). This reversed interval encompasses the *Chiasmolithus gigas* Subzone of Bukry (1975), which Jan Back-

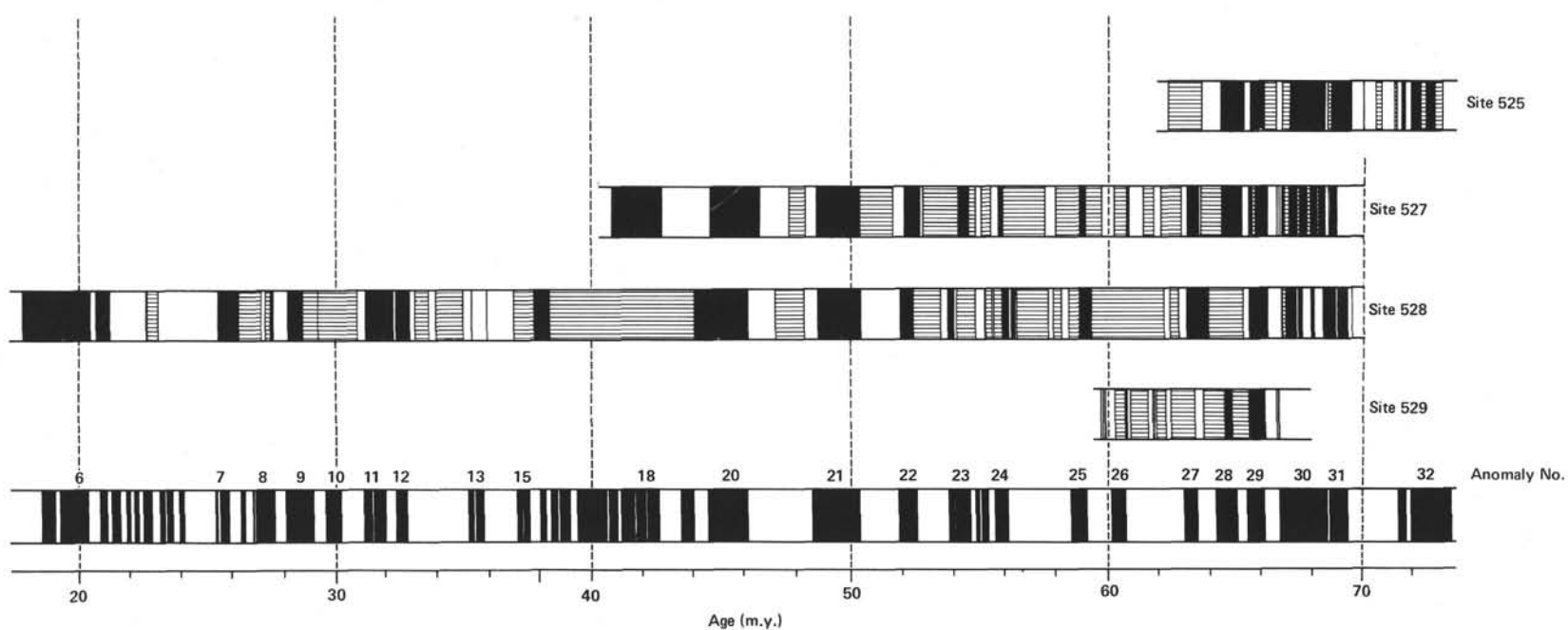


Figure 2. Interpreted magnetic data for Sites 525, 527, 528, and 529, plotted against inferred age. The magnetic reversal boundaries have been assigned ages from Kent (in press). All control points used are listed in Table 1. For comparison, the complete record as dated by Kent (in press) is indicated at the bottom of the figure. (Black, normal; white, reversed; lines, no data [disturbed or unrecovered] or not interpreted [low inclination].)

man (pers. comm., 1982) has found to be entirely contained by the reversed interval between Cores 16 and 17 in Site 527. Thus despite the spotty recovery of Anomalies 23 and 24 we are confident that the identification of the magnetostratigraphy up to Anomaly 20 is correct. By referring to the data in Tauxe et al. (in press) it is also possible to identify the anomalies in the Oligocene with reasonable confidence, although other interpretations of the sequence are possible.

ACCUMULATION RATES

Figure 3 shows accumulation rates for Sites 525 to 529 using the timescales discussed above (from Table 3). All data are in g/cm^2 per 10^3 y ., using shipboard density data. In view of the scattered measurements of wet-

water content and bulk density, averages were taken over several cores at a time. It should be remarked that uncertainties from this source are very small compared with all others entering in this chapter. Generally gravimetric data were used in preference to GRAPE data.

Accumulation rates have been expressed over million-year intervals. Since the ages of biostratigraphic datums have not been rounded to the nearest million years, as was general practice until recently, the procedure adopted has the advantage of slightly reducing the random fluctuations in apparent accumulation rate that arise from the uncertainty in the positioning of each datum. Because we have no good evidence for major sedimentological changes at any boundary except at the end of the Cretaceous, there is no advantage to be

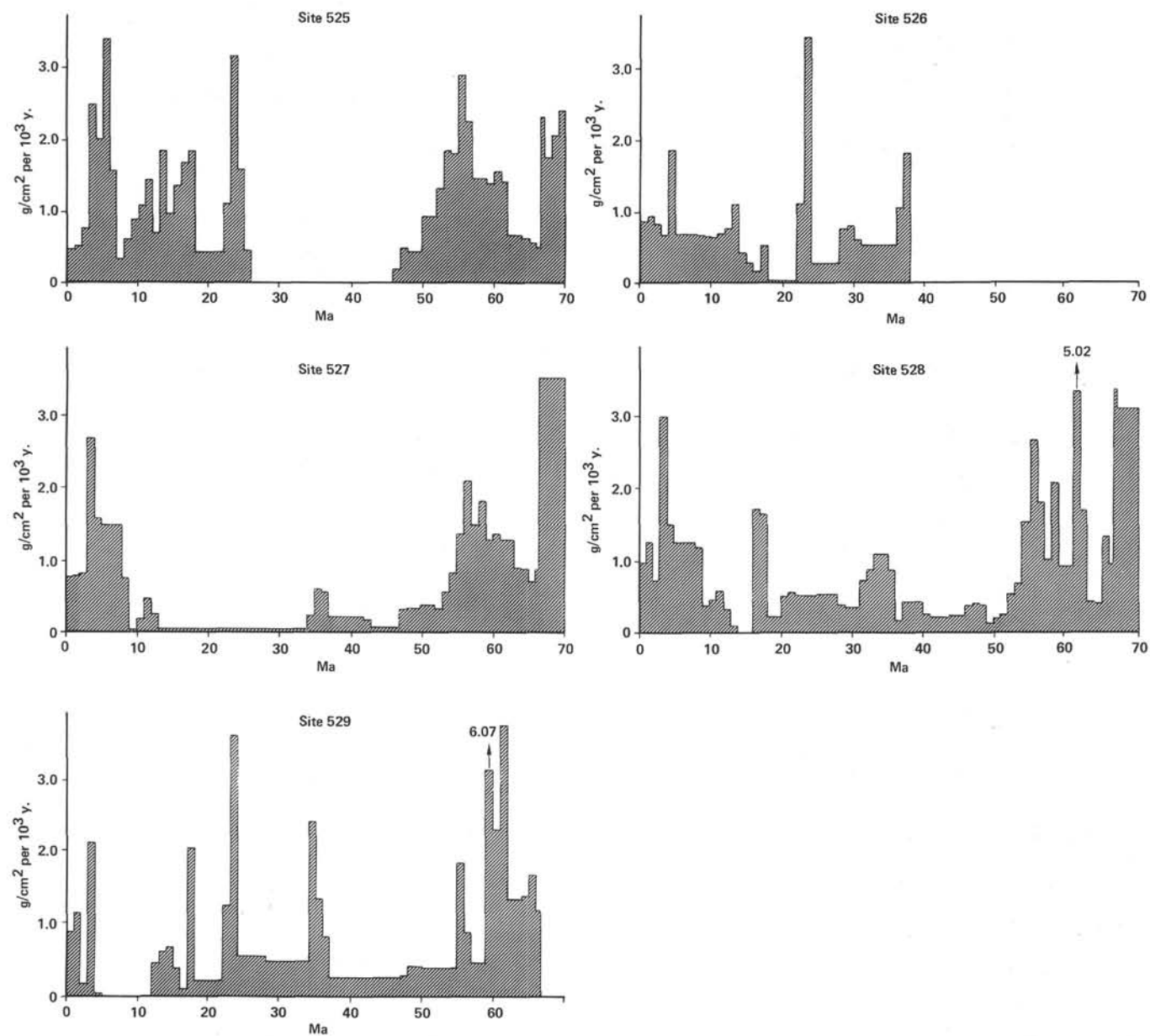


Figure 3. Accumulation rates for Sites 525–529 estimated in million-year increments. Age control points are from Table 1. For Site 528, the off-scale value is due to slumping. At Site 529, slumping was noted in several intervals in addition to the one that shows off-scale.

Table 3. Depth (in m) of interpolated m.y. points in Leg 74 sites, using Table 1 controls.

Age (m.y.)	Site 525	Site 526	Site 527	Site 528	Site 529
1	4.89	8.15	7.37	8.86	7.62
2	10.05	16.98	14.99	20.38	17.43
3	17.51	24.81	22.78	27.17	18.90
4	39.36	30.70	45.68	52.92	37.23
5	57.00	47.20	59.10	65.65	37.45
6	85.64	53.11	71.96	76.28	37.45
7	98.93	59.01	84.83	86.91	37.45
8	101.98	64.92	97.69	97.54	37.45
9	107.35	70.78	104.22	10.29	37.46
10	115.06	76.59	104.43	107.17	37.46
11	124.78	82.84	106.27	110.74	37.46
12	137.52	89.73	110.55	115.34	37.46
13	143.83	97.34	113.02	117.89	41.37
14	160.03	108.41	113.05	118.50	46.58
15	168.60	112.56	113.09	118.50	52.36
16	179.64	115.30	113.13	118.51	55.64
17	193.15	116.65	113.17	132.20	56.43
18	207.95	121.08	113.21	145.21	74.05
19	211.87	121.27	113.25	146.80	75.72
20	215.78	121.46	113.28	148.39	77.38
21	219.70	121.65	113.32	152.29	79.05
22	223.62	121.85	113.36	156.65	80.72
23	233.69	131.52	113.40	160.74	91.17
24	260.77	160.99	113.44	164.83	120.29
25	274.48	163.24	113.47	168.92	124.65
26	278.60	165.48	113.51	173.05	129.00
27		167.73	113.55	177.24	133.36
28		169.98	113.59	181.43	137.71
29		175.89	113.63	184.35	141.53
30		182.20	113.66	187.05	145.28
31		186.93	113.70	189.74	149.04
32		190.98	113.74	195.43	152.79
33		195.03	113.78	212.22	156.54
34		199.08	113.82	210.78	160.30
35		203.12	115.90	219.35	181.37
36		207.17	121.05	226.15	192.93
37		215.13	125.86	227.33	200.00
38		228.97	127.69	230.70	202.15
39			129.51	234.08	204.29
40			131.33	237.45	206.43
41			133.16	239.53	208.58
42	278.61	134.98	241.28	210.72	
43	279.04	136.45	243.04	212.86	
44	278.82	136.97	244.79	215.01	
45	278.93	137.49	246.54	217.15	
46	297.04	138.02	248.29	219.29	
47	280.70	138.54	251.09	221.44	
48	284.60	141.33	254.25	223.86	
49	288.12	144.18	257.24	227.43	
50	291.65	147.10	257.99	231.00	
51	298.92	150.34	259.31	234.23	
52	306.19	153.68	260.93	237.46	
53	315.98	156.40	264.76	240.69	
54	329.55	160.80	269.50	243.92	
55	342.77	166.71	280.43	247.15	
56	363.94	177.80	299.51	260.50	
57	380.41	192.11	312.27	266.77	
58	391.15	206.42	319.33	270.01	
59	401.88	220.47	334.13	273.25	
60	412.11	230.43	340.41	310.98	
61	423.59	240.20	346.70	325.30	
62	433.95	249.34	379.70	348.70	
63	438.16	258.48	390.60	357.01	
64	442.56	264.84	393.40	365.32	
65	446.56	271.52	398.05	373.88	
66	450.21	276.93	404.32	384.37	
66.46	451.71	280.00	407.00	387.77	
67	459.55	292.89	418.35		
68	470.53	317.06	437.61		
69	483.46	341.23	456.87		
70	498.61	365.40	476.13		

Note: Since these are m.y. intervals, the difference between adjacent depths is identical with the mean accumulation rate over that interval.

gained by estimating accumulation rates zone by zone. At this latter boundary an extra division has been inserted at 66.46 Ma, because it is certain that there was a change in accumulation rate more or less precisely associated with that boundary (Chave, this vol.).

Noncarbonate Accumulation Rates

In Appendix A the shipboard carbonate data are assigned ages on the basis of the control points in Table 1. For each site these data are shown as a function of age in Figure 4, which gives a general idea of changing dis-

solution at the various sites. For every million-year increment in which one or more shipboard carbonate determinations has been made, the accumulation of the noncarbonate fraction was determined by multiplying total accumulation by the noncarbonate fraction. These data are given in Table 4. Where no determination was available, an estimate was made on the basis of nearby values if this seemed appropriate. Figure 5 shows the noncarbonate accumulation averaged for all sites over each million-year increment. It should be noted that here and elsewhere we have not taken account of zeros in taking the mean. Our aim is to obtain the best estimate of the noncarbonate flux; if one intends to compile an ocean budget one must take account of hiatuses in a rather different manner. For the Plio-Pleistocene, the average accumulation rate is 0.055 g/cm² per 10³ y.; for the Miocene, it is 0.047, for the Oligocene, 0.058, and for the Eocene, 0.055. These figures are essentially indistinguishable, which is surprising in the light of the recent global compilation of Al accumulation by Donnelly (1982), which shows a significant increase in the late Neogene. Although taking shorter time intervals suggests changes in the noncarbonate accumulation rate, it is quite possible that these are all artifacts of errors in the timescale.

Two potentially very interesting episodes are the apparent rises in noncarbonate accumulation between 13 and 11 Ma in Site 527, and between 36 and 34 Ma. Both of these may be associated with glaciation in Antarctica. The first episode, in the Miocene, is critically dependent on the ages of the limits of Zones NN8 and NN9. The limits assigned are 12.8 to 12.0 Ma and 12.0 to 10.6 Ma. During this interval the CCD deepened briefly from a position between 4000 and 4400 m to about 4400 m, permitting the identification of key nannofossil species in Hole 527 sediment (Jiang and Gartner, this volume); however, in such dissolved material this estimate of accumulation rate remains hazardous. The episode of higher noncarbonate accumulation in the early Oligocene is controlled by the limits of Anomaly 13 in Site 528 sediments, as well as by nannofossils at Sites 529 and 527; in Hole 527, the presence of normal magnetization in Core 14 is inconsistent with the biostratigraphic age assignment, so the estimate may be unreliable. More work should be done to ascertain whether these peaks in noncarbonate accumulation are real, or whether they are artifacts caused by the difficulties that have been mentioned earlier.

Within the Eocene, there is apparently a contrast between lower noncarbonate accumulation in the lower and middle Eocene, and higher accumulation in the upper Eocene. This indication should be treated with caution, because the age controls used for the late Eocene are subject to considerable uncertainties at present. At the same time it is interesting, because superficially it appears that the late Eocene is missing through erosion at all sites. On the other hand, the sediment recovered is all very low in carbonate, and the quantity of noncarbonate turns out to be more than enough to imply that in reality accumulation at Sites 529, 528, and 527 was continuous. Since there is certainly no late Eocene sedi-

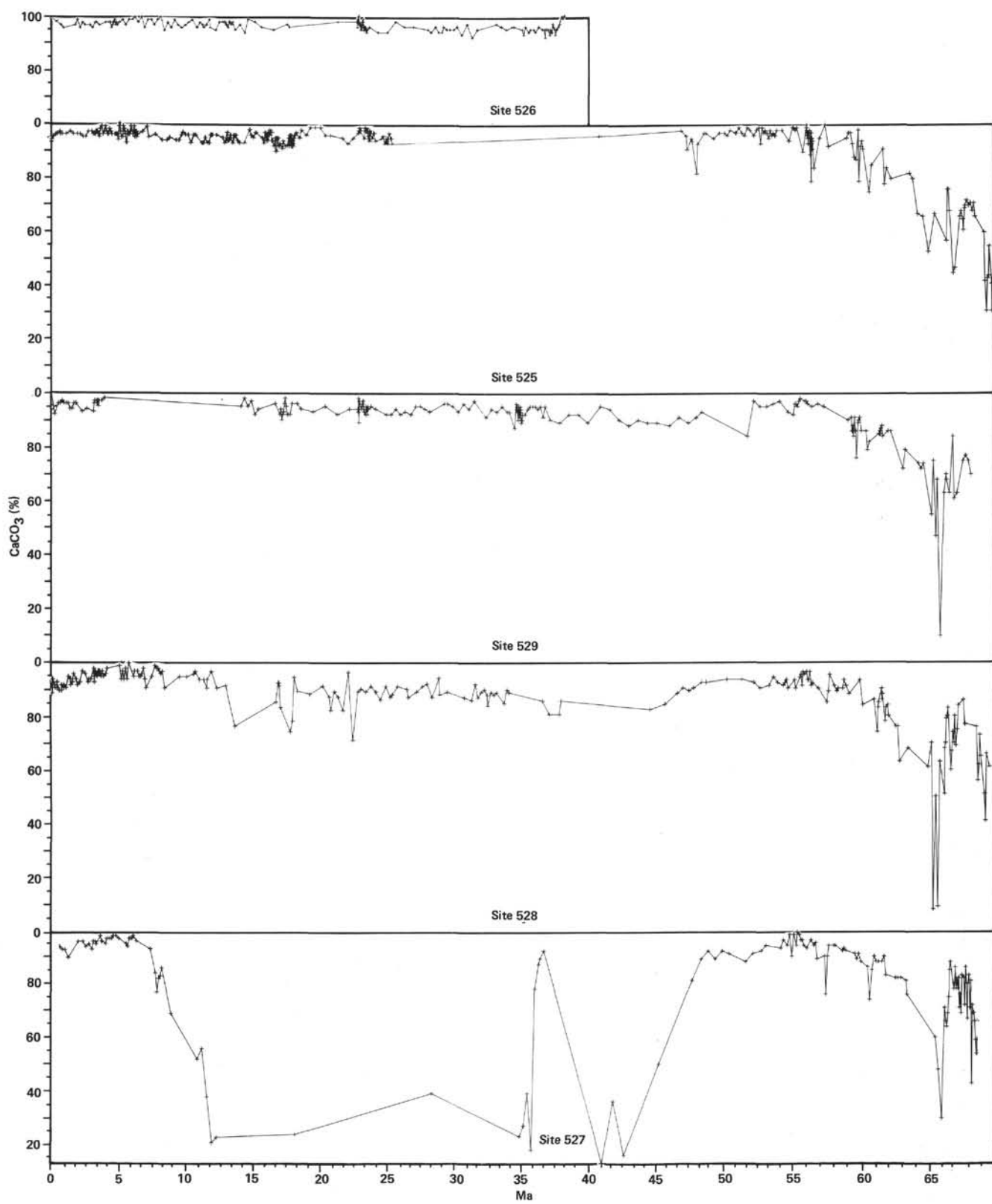


Figure 4. Carbonate content for Leg 74 sites, plotted against age using the control points of Table 1. The carbonate data are from shipboard measurements.

Table 4. Accumulation rates (g/cm^2 per 10^3 y) of noncarbonate fraction in Leg 74 sites.

Time Increment (m.y.)	Site 526	Site 525	Site 529	Site 528	Site 527	Mean Accumulation
0-1	0.030	0.022	0.045	0.094	0.051	0.048
1-2	0.028	0.020	0.058	0.096	0.067	0.054
2-3	0.021	0.033	0.012	0.048	0.038	0.030
3-4	0.018	0.085	0.075	0.151	0.116	0.089
4-5	0.044	0.070	H	0.045	0.048	0.052
5-6	0.011	0.112	H	0.055	0.059	0.059
6-7	0.005	0.055	H	0.071	0.094	0.056
7-8	0.013	0.012	H	0.045	0.237	0.077
8-9	0.018	0.036	H	0.074	0.156	0.071
9-10	0.018	0.042	H	0.022	H	0.027
10-11	0.016	0.052	H	0.024	0.096	0.047
11-12	0.019	0.081	H	0.041	0.288	0.11
12-13	0.020	0.040	0.02*	0.030	0.207	0.063
13-14	0.033	0.096	0.03*	H	H	0.053
14-15	0.014	0.044	0.034	H	H	0.031
15-16	0.008	0.065	0.030	H	H	0.034
16-17	0.008	0.101	0.004	H	H	0.038
17-18	0.018	0.122	0.103	H	H	0.081
18-19	0.001*	0.016	0.008	H	H	0.005
19-20	0.001*	0.005	0.01*	H	H	0.003
20-21	0.001*	0.018	0.010	0.062	H	0.023
21-22	0.001*	0.023	0.017	0.064	H	0.026
22-23	0.021	0.037	0.095	0.043	H	0.049
23-24	0.132	0.98	0.235	0.051	H	0.129
24-25	0.015	0.089	0.04*	0.058	H	0.051
25-26	0.010	H	0.043	0.060	H	0.038
26-27	0.010	H	0.033	0.051	H	0.031
27-28	0.010	H	0.033	0.051	H	0.031
28-29	0.038	H	0.02*	0.037	H	0.032
29-30	0.039	H	0.022	0.037	H	0.033
30-31	0.031	H	0.026	0.044	H	0.034
31-32	0.026	H	0.019	0.082	H	0.046
32-33	0.03*	H	0.035	0.104	H	0.056
33-34	0.020	H	0.030	0.125	H	0.058
34-35	0.020	H	0.169	0.1*	0.19	0.12
35-36	0.026	H	0.067	0.1*	0.43	0.16
36-37	0.055	H	0.048	0.02	0.075	0.050
37-38	0.089	H	0.026	0.073	0.14*	0.082
38-39	H	0.02*	0.04*	0.15*	H	0.07*
39-40	H	0.02*	0.04*	0.15*	H	0.07*
40-41	H	0.02*	0.04*	0.18	H	0.08*
41-42	H	0.02*	0.04*	0.14	H	0.07*
42-43	H	0.02*	0.04*	0.14	H	0.07*
43-44	H	0.02*	0.04*	0.03*	H	0.03*
44-45	H	0.02*	0.037	0.03*	H	0.03*
45-46	H	0.02*	0.036	0.031	H	0.03
46-47	0.004	0.023	0.035	0.03*	H	0.023
47-48	0.043	0.03*	0.037	0.061	H	0.043
48-49	0.020	0.03*	0.025	0.031	H	0.027
49-50	0.018	0.03*	0.005*	0.032	H	0.021
50-51	0.029	0.03*	0.011	0.034	H	0.026
51-52	0.021	0.03*	0.014	0.046	H	0.038
52-53	0.040	0.031	0.042	0.027	H	0.035
53-54	0.060	0.016	0.044	0.034	H	0.039
54-55	0.072	0.027	0.114	0.039	H	0.063
55-56	0.087	0.064	0.148	0.060	H	0.090
56-57	0.124	0.032	0.107	0.142	H	0.101
57-58	0.063	0.025	0.091	0.187	H	0.092
58-59	0.08*	0.03*	0.173	0.119	H	0.101
59-60	0.090	S	0.083	0.119	H	0.097
60-61	0.22	S	0.09	0.21	H	0.17
61-62	0.22	S	S	0.19	H	0.20
62-63	0.12	0.19	S	0.23	H	0.12
63-64	0.12	0.34	0.14	0.18	H	0.20
64-65	0.19	0.37	0.14*	0.24*	H	0.24
65-66	0.23	0.66	0.78	0.32	H	0.50
66-66.46	0.10	0.43	0.39	0.43	H	0.34
66.46-67	0.54	H	0.86	0.89	H	0.76
67-68	0.68	H	0.71	0.75	H	0.71
68-69	0.63	H	0.90	1.11	H	0.88
69-70	1.37	H	1.20	1.29	H	

Note: * = estimates in time increments for which no carbonate data are available; figure has been interpolated from nearby values; H = increments during which site is reported to have experienced a hiatus in accumulation; S = presence of a significant amount of slumped material.

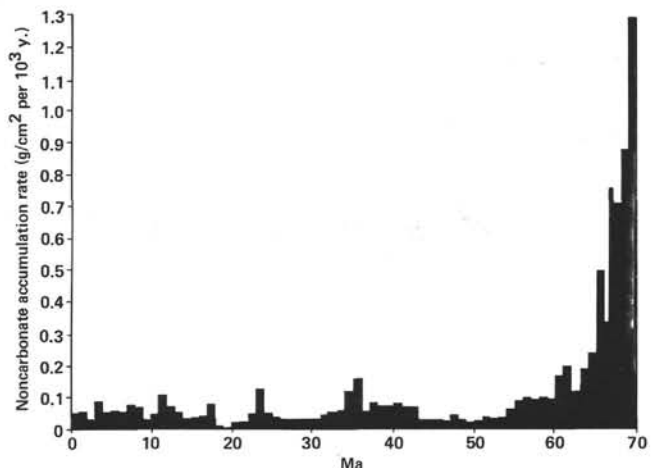


Figure 5. Average accumulation rate of the noncarbonate content at Sites 525-529, obtained from the total accumulation rate and the noncarbonate percentage (from Table 4).

ment preserved at the shallower Site 525, which must have been eroded, we do not know what the nannofossil rain rate was during this interval. Presumably as a result of dissolution, the actual average nannofossil accumulation was very low (approximately $0.2 \text{ g}/\text{cm}^2$ per 10^3 y) at Sites 529, 528, and 527, and it is impossible to deduce what proportion of the nannofossils falling from the photic zone this represents.

In the Palaeocene and Maestrichtian, noncarbonate input was presumably enhanced by proximity to the ridge crest, since noncarbonate accumulation fell rather smoothly from over $1 \text{ g}/\text{cm}^2$ per 10^3 y . between 70 and 69 Ma to the "steady-state" value of about $0.06 \text{ g}/\text{cm}^2$ per 10^3 y . in the Eocene (Figure 5).

An examination of the noncarbonate accumulation rate for each site reveals an increase from the shallower to the deeper sites. The mean noncarbonate accumulation at Site 526 at 1000 m water depth is about $0.25 \text{ g}/\text{cm}^2$ per 10^3 y ; at the intermediate Sites 525 and 529, at 2500 and 3000 m, the mean is about $0.45 \text{ g}/\text{cm}^2$ per 10^3 y ., and in the deeper Sites 528 and 527 at 4000 and 4400 m, the mean is about $0.6 \text{ g}/\text{cm}^2$ per 10^3 y . Recent work on the accumulation on sediment traps (Honjo et al., 1982) deployed at different depths shows a similar increase with depth in the accumulation of the terrigenous flux.

Nannofossil and Foraminiferal Accumulation Rates

For every million-year increment from which one or more sample has been sieved either in Cambridge (NJS) or in Kiel (DF), a separation was made to show the accumulation of sediment $>$ and $<$ $63 \mu\text{m}$. The data are shown in Appendix B as a function of estimated age, using the control points in Table 1. Figure 6 shows the coarse-fraction percentage as a function of age for each site and like Figure 4 gives a rough picture of dissolution history. The coarse fraction is essentially 100% foraminifers in virtually all samples. A few samples in the lowest parts of Sites 525 and 528 are too lithified to make a useful separation, so that the high values should be disregarded. We have assumed that the noncarbonate

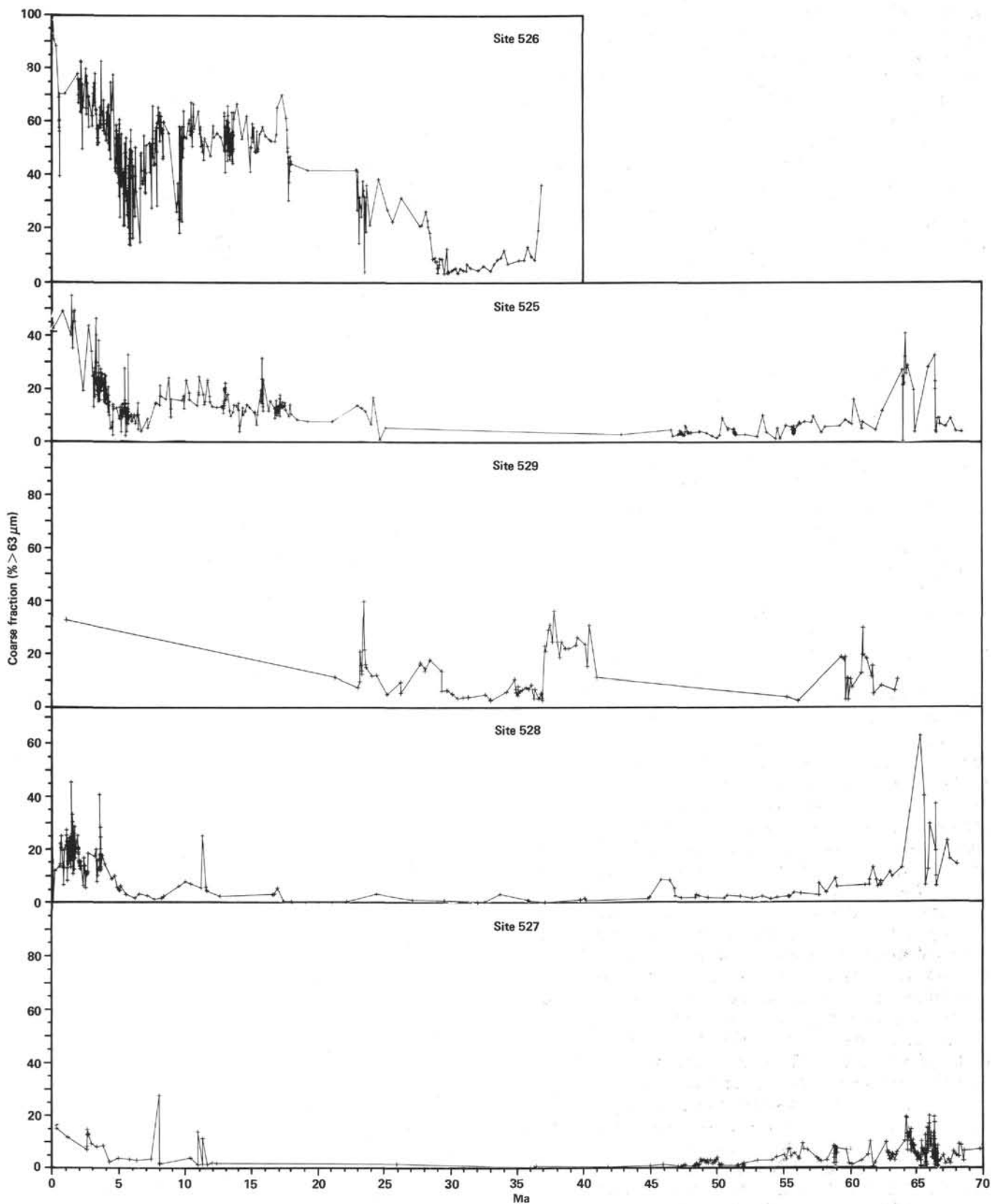


Figure 6. Percentage of the coarse fraction ($>63 \mu\text{m}$) at Leg 74 sites. The data are from Borella (this volume) and from measurements made in Cambridge and aboard ship by Shackleton (Table 3). Estimated age derived from Table 1.

portion is all in the fine fraction and have estimated nannofossil accumulation as total fine-fraction accumulation minus noncarbonate accumulation. Examination of smear slides shows that in the shallowest site, 526, the fine fraction contains a significant proportion of small foraminifers and foraminiferal fragments, so that the true nannofossil accumulation at Site 526 is even less than indicated. Fine-fraction carbonate accumulation rates are given in Table 5 (by subtracting the coarse-fraction rate from the total carbonate rate), and coarse-fraction rates in Table 6. Since dissolution varies considerably, it was not considered useful to interpolate values for Table 6, although interpolated coarse-fraction values were in some cases (marked with asterisks) used for Table 5. (Since the coarse fraction seldom exceeds 10% in much of the record, an estimated figure does not contribute much uncertainty to the estimate of the fine fraction.)

Figure 7 shows the accumulation rate of the coarse fraction and of the carbonate fine fraction, averaged in million-year increments, at each site. This figure contains information on the history of production rates of foraminifers and coccoliths as a function of time. It also contains information on the changing vertical gradient of calcite dissolution and winnowing, which may be deduced from differences among sites in the accumulation rates of each component.

Table 5 also illustrates the effect of winnowing on the shallower sites. Column 7 ("deep mean") shows the mean nannofossil accumulation rate over the deeper sites. For the Neogene, this represents the average for Sites 525, 529, 528, and 527 (values severely affected by dissolution are neglected). For the Paleogene, this column encompasses Sites 529, 528, and 527. The last column shows the ratio of nannofossil accumulation in the shallowest site to this mean. From the Oligocene up to the present the shallowest site is 526; in the earlier part of the record, when Site 526 was probably near or above sea level, it is Site 525. For the Neogene, the ratio averages about 0.35, and for the Oligocene about 0.8; although Site 526 was shallower early in the Oligocene, winnowing only began to have a really significant effect later in the Oligocene, probably at about 28 Ma.

It appears that Site 525 experienced considerable winnowing in the Maestrichtian and early Paleocene, with a sudden decrease in winnowing at 62 Ma. Over this interval, the nannofossil accumulation at Site 525 was about half the mean for the deeper sites. During the remainder of the Paleocene there is little difference among sites, but in the Eocene the nannofossil accumulation is actually higher at Site 525 than in the deeper sites. Although there were some foraminifers preserved even in Site 527, it seems that dissolution was taking its toll on the nannofossils. In view of the prevalence of slumping, little work has been done on Site 529, and it is not certain that the nannofossils were being significantly dissolved at this site. Certainly, there was a typical nannofossil dissolution loss of the order of 50% at Sites 528 and 527 in the Eocene.

Figure 8 shows the accumulation rate of foraminifers versus paleo-water depth for a few selected intervals.

Table 5. Accumulation rate of the nannofossil fraction in Leg 74 sites.

Time Increment (m.y.)	Site 526	Site 525	Site 529	Site 528	Site 527	Deep Mean ^a	Shallow/ Deep ^b
0-1	0.25	0.26	0.78	0.71	0.60	0.59	0.42
1-2	0.21	0.51	0.97	0.89	0.63	0.75	0.28
2-3	0.23	0.51	0.14*	0.60	0.68	0.48	0.48
3-4	0.23	1.84	1.79	2.33	2.36	2.08	0.11
4-5	0.84	1.69	H	1.33	1.48	1.50	0.56
5-6	0.40	2.91	H	1.12	1.37	1.80	0.22
6-7	0.39	1.38	H	1.14	1.39	1.30	0.30
7-8	0.31	0.31	H	1.15	1.19	0.88	0.35
8-9	0.28	0.50	H	1.08	0.58	0.72	0.39
9-10	0.35	0.74	H	0.31	D	0.52	0.67
10-11	0.24	0.85	H	0.40	0.09	0.58	0.41
11-12	0.31	1.12	H	0.49	0.17	0.81	0.38
12-13	0.33	0.56	0.39*	2.28	0.06	1.08	0.31
13-14	0.48	1.52	0.53*			H	1.03
14-15	0.20	0.83	0.60			H	0.72
15-16	0.12	1.09	0.32*			H	0.72
16-17	0.06	1.38	0.1*			H	0.74
17-18	0.24	1.48	1.84			H	1.66
18-19	0.01*	0.39	0.2*			H	0.29
19-20	0.01*	0.41	0.2*			H	0.31
20-21	0.01*	0.40	0.2*	0.43*		H	0.34
21-22	0.01	0.40	0.2*	0.49*		H	0.36
22-23	0.73	0.94	1.07	0.47*		H	0.83
23-24	2.38	2.74	2.72	0.45*		H	1.97
24-25	0.14	1.36	0.44*	0.43		H	0.74
25-26	0.18	0.43	0.47	0.46*		H	0.45
26-27	0.17	H	0.46	0.46*		H	0.46
27-28	0.20	H	0.42	0.47		H	0.45
28-29	0.60	H	0.36*	0.32*		H	0.34
29-30	0.69	H	0.42	0.30		H	0.36
30-31	0.53	H	0.42	0.30*		H	0.36
31-32	0.45	H	0.43	0.73		H	0.58
32-33	0.44	H	0.41	0.74		H	0.58
33-34	0.45	H	0.41*	0.94		H	0.68
34-35	0.42	H	2.09	0.94	0.16*	1.51	0.28
35-36	0.88	H	1.18	0.72*	0.52*	0.81	1.1
36-37	1.22	H	0.72	0.12*	0.48	0.44	2.8
37-38		H	0.15	0.35*	0.05*		
38-39		H	0.17	0.35*	0.05*		
39-40		H	0.2*	0.2*	0.05*		
40-41		H	0.2*	0.2*	0.05*		
41-42		H	0.2*	0.2*	0.05*		
42-43		H	0.2*	0.2*	0.05*		
43-44		H	0.2*	0.2*	0.03*		
44-45		H	0.2*	0.2*	0.03*		
45-46		H	0.2*	0.2*	0.03*		
46-47		0.21	0.2*	0.31	0.03	0.25	0.8
47-48		0.45	0.21*	0.35	0.26	0.27	1.7
48-49		0.42	0.3*	0.33	0.29	0.31	1.4
49-50		0.43	0.3*	0.10	0.30	0.23	1.9
50-51		0.87	0.3*	0.17	0.34	0.27	3.2
51-52		0.90	0.3*	0.21	0.34	0.28	3.2
52-53		1.25	0.3*	0.48	0.28	0.35	3.6
53-54		1.70	0.3*	0.60	0.52	0.47	3.6
54-55		1.69	0.3*	1.38	0.75	0.81	2.1
55-56		2.69	1.77	2.43	1.25	1.82	1.5
56-57		1.98	0.86	1.61	1.86	1.44	1.4
57-58		1.31	0.4*	0.86	1.26	0.84	1.6
58-59		1.30	0.4*	1.76	1.61	1.26	1.0
59-60		1.21	S	0.74	1.03	0.87	1.4
60-61		1.21	S	0.74*	1.13	0.94	1.3
61-62		1.13	S	S	1.04	1.04	1.1
62-63		0.49	1.23	1.21	0.98	1.14	0.4
63-64		0.38	1.23	0.23	0.68	0.71	0.5
64-65		0.31	0.9*	0.21*	0.54	0.55	0.6
65-66		0.19	0.9*	0.14	0.34	0.46	0.4
66-66.46		0.29	0.7*	0.27	0.36	0.44	0.7
66.46-67		1.63		2.22	2.48	2.35	0.7
67-68		0.95		1.75	2.68	2.2	0.4
68-69		1.24		0.75	2.22	1.49	0.8

Note: This accumulation rate is obtained as (total accumulation rate) - (coarse-fraction accumulation rate) - (noncarbonate accumulation rate).

* = estimate where coarse-fraction and/or carbonate data are missing; figure has been interpolated from neighboring values. H = hiatus; S = presence of a significant amount of slumped material.

^a Mean nannofossil accumulation rate over the deeper sites (see text for further explanation).

^b Ratio of nannofossil accumulation in the shallowest site to the deep mean (see text for further explanation).

Table 6. Accumulation rate ($\text{g}/\text{cm}^2 \text{ per } 10^3 \text{ y.}$) of the foraminiferal fraction ($> 63 \mu\text{m}$).

Time Increment (m.y.)	Site 526	Site 525	Site 529	Site 528	Site 527
0-1	0.58	0.23	0.064	0.17	0.116
1-2	0.69	0.24	0.12	0.27	0.093
2-3	0.57	0.24		0.093	0.090
3-4	0.41	0.56	0.27	0.53	0.227
4-5	0.97	0.25	H	0.11	0.051
5-6	0.25	0.39	H	0.059	0.052
6-7	0.26	0.14	H	0.032	0.046
7-8	0.34	0.04	H	0.025	0.053
8-9	0.36	0.10	H	0.023	0.014
9-10	0.28	0.14	H	0.026	H
10-11	0.37	0.21	H	0.032	0.005
11-12	0.36	0.25	H	0.053	0.008
12-13	0.41	0.12	0.046	0.007	0.005
13-14	0.60	0.23			H
14-15	0.21	0.11	0.048		H
15-16	0.15	0.22			H
16-17	0.09	0.21		0.062	H
17-18	0.25	0.25	0.12	0.007	H
18-19	0.01*	0.04			H
19-20	0.01	0.03			H
20-21	0.01*	0.03			H
21-22	0.01*	0.03	0.02		H
22-23	0.36	0.15	0.09		H
23-24	0.88	0.33	0.65		H
24-25	0.10	0.14	0.063	0.016	H
25-26	0.068	0.03	0.026		H
26-27	0.081	H	0.040		H
27-28	0.053	H	0.087	0.004	H
28-29	0.089	H	0.075		H
29-30	0.044	H	0.029	0.002	H
30-31	0.025	H	0.020		H
31-32	0.021	H	0.018	0.001	H
32-33	0.019	H	0.016	0.001	
33-34	0.035	H		0.033	
34-35	0.033	H	0.162		
35-36	0.046	H	0.084	0.007	
36-37	0.089	H	0.038		0.002
37-38	0.47	H	0.068	0.0004	
38-39		H	0.055		
39-40		H	0.061		
40-41		H	0.050		
41-42		H			
42-43		H			
43-44		H			
44-45		H			
45-46		H		0.0005	
46-47		0.007			
47-48		0.019		0.002	
48-49		0.018		0.005	
49-50		0.014		0.002	0.008
50-51		0.045		0.004	0.005
51-52		0.035		0.005	0.003
52-53		0.049		0.008	0.003
53-54		0.10		0.016	0.014
54-55		0.05		0.026	0.026
55-56		0.12	0.066	0.072	0.070
56-57		0.16	0.01	0.062	0.120
57-58		0.10		0.050	0.042
58-59		0.09		0.134	0.088
59-60		0.10		0.052	0.070
60-61		0.14			0.023
61-62		0.07			0.052
62-63		0.08	0.11	0.12	0.074
63-64		0.19	0.11	0.049	0.035
64-65		0.14			0.085
65-66		0.16		(0.40)	0.041
66-66.46		0.13		(0.27)	0.080
66.46-67		0.16	H	(0.28)	0.115
67-68		0.13	H	(0.61)	0.102
68-69		0.20	H	(1.4)	(0.194)

Note: Figures in brackets are probably invalid because sediment is partially lithified. H = hiatus. * = interpolated values for the % $> 63 \mu\text{m}$. A blank is left where it was judged that an interpolated value would not be sufficiently accurate.

This figure illustrates the fact that the total flux of material from the surface layers is not generally recorded at any site. The foraminiferal flux is best recorded at the shallow Site 526, but the nannofossil flux is best recorded at an intermediate site, one that is well above the CCD to avoid dissolution effects, but away from topographic highs to avoid winnowing. Thus in attempting to estimate the total amount of internal carbonate recycling in the ocean that results from the precipitation of calcite in surface waters and its dissolution in deeper waters, one needs data from several water depths. The Leg 74 sites constitute a unique data set for such studies.

It is interesting to observe in Figure 8 the enormous loss of foraminifers between the shallowest Site 526 and Site 525; although the seafloor at Site 525 is well above the lysocline as generally understood, it has experienced about 50% loss of the foraminiferal flux by dissolution. To examine this feature, several samples were sieved further into size classes, showing that it was mainly the very small foraminifers that accumulated at Site 526 but were dissolved on the seafloor at Site 525.

In their classic study of carbonate distribution and dissolution in the equatorial Pacific, van Andel et al. (1975) were obliged to assume that the carbonate rain rate was well estimated by the accumulation rate at the site of their shallowest cores. The present data suggest that the true carbonate rain rate must have been higher. If half the foraminiferal rain rate in the South Atlantic (CCD about 4400 m) is dissolved at 2500 m, the loss must be considerably greater at that depth in the Pacific.

Winnowing

Our data indicate a gradual increase with depth in the accumulation rate of both the fine fraction and the non-carbonate fraction. These figures may be compared with the data obtained by Honjo et al. (1982) from sediment trap studies. In addition, however, the fine-fraction accumulation rate in Site 526 is very considerably reduced by comparison with the deeper sites; this we interpret as the result of winnowing. It seems that the magnitude is underestimated by our crude methods, since an examination of the fine fraction from Site 526 reveals that it contains a large proportion of whole and broken very small foraminifers, so that the coccolith accumulation is even less than indicated by the $< 63 \mu\text{m}$ accumulation.

Fish Tooth Accumulation

It is clear from this discussion that if dissolution is pervasive at almost all depths, even when the CCD is very deep, then it is difficult to use foraminiferal accumulation as a measure of marine productivity even when relatively shallow sites are available. For this reason, we have experimented with measuring the accumulation rate of fish teeth. Fish teeth (or ichthyoliths) are very resistant to solution, and indeed are now used as a biostratigraphic tool in red clay sequences (Doyle and Riedel, 1978). We were intrigued to notice the large fluctuations in ichthyolith accumulation during the Paleogene in the study of Core GPC5 (Doyle and Riedel, 1978), and we wondered whether this reflected changes in productivity rather than only resulting from the geo-

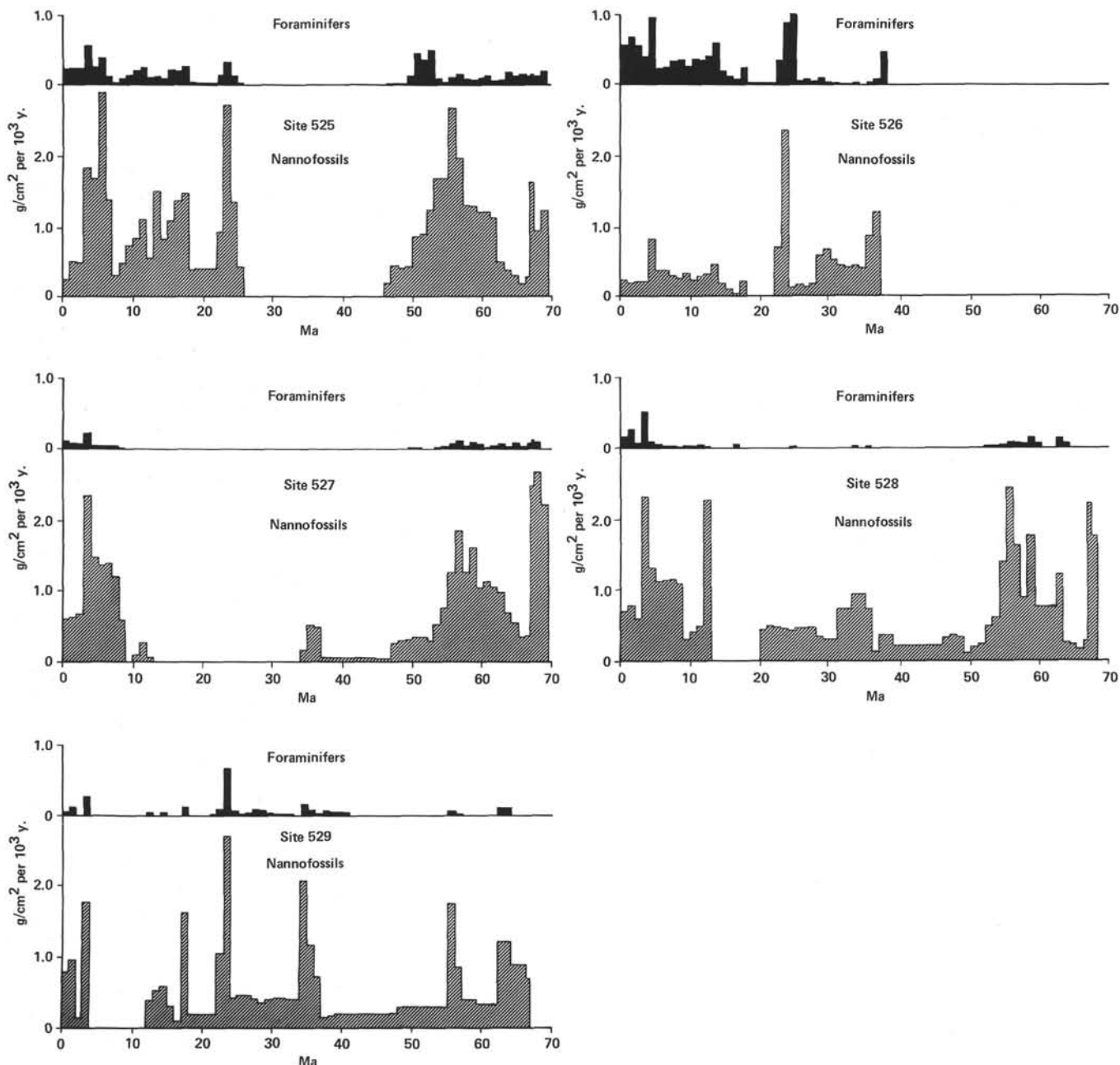


Figure 7. Accumulation rate of the foraminiferal fraction ($>63 \mu\text{m}$; above) and the nannofossil fraction ($<63 \mu\text{m}$, minus noncarbonate; below) at Leg 74 sites. Data from Appendix A.

graphical motion of the coring site, as Doyle and Riedel believed.

In Leg 74 samples, ichthyoliths were picked from the $>63 \mu\text{m}$ fraction in samples washed for oxygen isotope studies. The majority of specimens are smaller than $250 \mu\text{m}$, whereas the majority of foraminifers used for isotope analysis are larger. To utilize the material most effectively, our procedure was to search for ichthyoliths among the foraminifers in the $>250 \mu\text{m}$ fraction so as to preserve the foraminifers for future use, and to dissolve the foraminifers in the finer size fraction using acetic acid, since seeking fish teeth in this size fraction proved impossibly slow. Table 7 gives the total counts, the number/g sediment, and the estimated accumula-

tion rates; Table 8 shows the accumulation averaged in million-year increments. Figure 9 shows accumulation of ichthyoliths in million-year increments. Comparing Figure 9 with Figure 7, which shows accumulation rates of other components over the same time intervals, it is clear that the estimation of fish-tooth accumulation provides a very powerful tool for measuring productivity in a manner unaffected by carbonate dissolution.

The lack of similarity between the ichthyolith accumulation and that of the noncarbonate component shows conclusively that the ichthyolith curve is not a dissolution artifact. Comparison with the foraminiferal accumulation at the shallowest Site 525 shows a good relationship, but even at this site dissolution destroys the

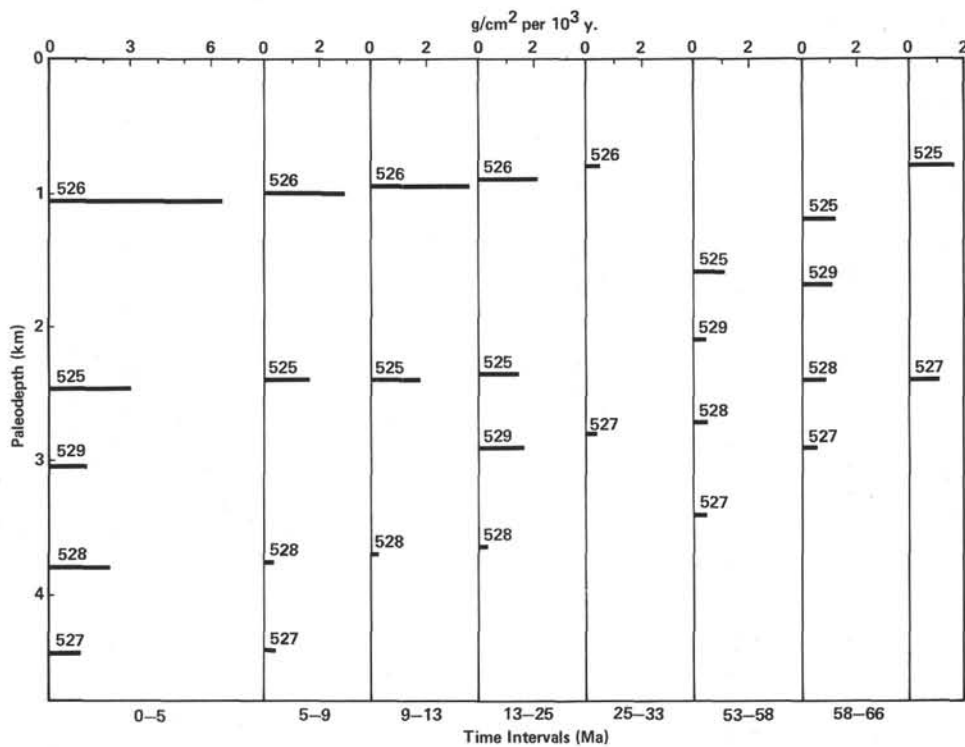


Figure 8. Accumulation of foraminiferal component as a function of paleodepth for the Leg 74 region.
For each site the data from Figure 7 and Appendix A are averaged over convenient intervals and plotted at approximately the paleodepth occupied by the site over that interval.

relationship as we come up through the middle Eocene. However, the record of ichthyolith accumulation does resemble that of nannofossil accumulation, suggesting that it is productivity, rather than deep-water chemistry, that controls the carbonate record. We believe that this shows a very promising opening for future work by making possible some estimate of marine productivity that is not biased by carbonate dissolution.

CONCLUSIONS

Accumulation of foraminiferal material, nannofossils, fish teeth, and noncarbonate residue were studied in the five sites drilled during Leg 74, on the premise that these sites monitor accumulation at different depths (and in different water masses) with identical rain rates from the surface. Accumulations have been computed in million-year intervals, which are certainly too short in relation to the limitations of present-day chronostratigraphy and drilling techniques in parts of the column; nevertheless, the results show that this resolution is both close to being attainable in much of the Cenozoic, and necessary for the portrayal of the timescale of change. In the earlier Paleogene in particular, accumulation rates were changing rapidly enough that a coarser resolution would conceal much of the picture.

At the Leg 74 Sites, noncarbonate input (in g/cm^2 per 10^3 y) fell smoothly from over 1 when the sites were close to the ridge crest 70 Ma, to about 0.03 in the Eocene and Oligocene, rising slightly in the late Neogene to an average of about 0.06. The number of fish teeth accumulating per $\text{cm}^2/10^3 \text{ y}$. (averaged over million-year intervals) was about 2.7 in the late Maestrichtian, falling

to 0.3 in the early Danian, rising to a maximum of 5.5 in the early Eocene, and falling to another minimum with typical values around 0.7 in the middle Eocene. Accumulation of carbonate (in g/cm^2 per 10^3 y) follows a similar pattern: nannofossil carbonate accumulation rates were about 2 in the Maestrichtian and at the early Eocene peak, falling below 0.7 in the early Danian and below 0.4 in the middle Eocene. Although the effect of increasing carbonate dissolution through the Eocene is clearly recorded by the comparison between accumulation rates of foraminiferal and nannofossil carbonate at different paleodepths, the fish-tooth data show that the underlying cause is changing productivity rather than changing oceanic deep-water chemistry.

Because of the lack of palaeomagnetic control on the Neogene sections drilled, accumulation-rate data are less reliable; some features are probably artifacts of the timescale employed. A peak in noncarbonate accumulation at about 13 Ma may result from Antarctic glaciation at that time. Late Neogene noncarbonate accumulation did not rise to the same extent as would be expected on the basis of global compilations.

Foraminiferal accumulation rates were studied at all sites. A consistent feature of the later Neogene is that about half the foraminiferal flux is dissolved at 2500 m, although this is well above the so-called lysocline; thus the concept of a foraminiferal lysocline is not supported by accumulation data. Nannofossil accumulation data show that winnowing has been very important at Site 526 (about 1 km depths) since some time in the middle Oligocene but that it was not during the earlier Oligocene. Winnowing has also affected Site 525 (about

Table 7. Accumulation of fish teeth in Maestrichtian to middle Eocene sediments at Site 527.

Sub-bottom Depth (m)	Total No. Teeth	Dry Wt. Raw Sediment (g)	Accumulation Rate		
			No. Teeth/g Sediment	Sediment ^a (g/cm ² per 10 ³ y.)	Fish Teeth (N/cm ² per 10 ³ y.)
138.71	74	14.58	5.08	0.323	1.64
142.27	23	10.30	2.23	0.329	0.73
143.77	24	12.35	1.94	0.329	0.64
146.77	26	11.57	2.25	0.339	0.76
152.28	4	7.85	0.51	0.386	0.20
153.78	35	15.07	2.32	0.316	0.73
156.78	29	9.25	3.14	0.563	2.37
161.50	29	12.51	2.32	0.756	1.75
167.50	15	8.67	1.73	1.374	2.38
168.91	73	14.27	5.12	1.374	7.03
171.71	23	13.71	1.68	1.374	2.31
175.65	19	11.23	1.69	1.374	2.32
180.17	24	11.95	2.01	2.118	4.26
184.71	34	10.68	3.18	2.118	6.74
199.81	8	11.69	0.68	1.494	1.02
204.31	24	14.85	1.62	1.494	2.42
218.14	6	5.65	1.06	1.832	1.94
218.34	7	7.51	0.93	1.832	1.70
218.63	13	7.90	1.65	1.832	3.02
220.21	13	8.26	1.57	1.832	2.88
221.11	21	8.02	2.62	1.276	3.34
227.85	20	12.19	1.64	1.276	2.09
232.15	10	12.61	0.79	1.366	1.08
239.21	16	9.97	1.60	1.366	2.19
243.71	10	8.85	1.13	1.280	1.45
245.21	24	14.65	1.64	1.280	2.10
256.31	17	8.82	1.93	1.280	2.47
260.17	14	9.49	1.48	0.891	1.31
261.10	10	8.38	1.19	0.891	1.06
266.35	20	11.09	1.80	0.869	1.56
267.79	18	7.56	2.38	0.869	2.07
269.44	13	11.80	1.10	0.869	0.96
271.11	26	15.25	1.70	0.869	1.48
272.35	10	15.62	0.64	0.703	0.45
276.21	1	2.98	0.34	0.703	0.24
277.42	8	8.83	0.91	0.868	0.79
277.94	10	7.22	1.39	0.868	1.20
278.35	4	7.31	0.55	0.868	0.47
279.06	13	7.46	1.74	0.868	1.51
279.71	8	4.46	1.26	0.868	1.09
280.68	6	4.00	1.50	3.485	5.23
281.40	1	3.52	0.28	3.528	0.99
294.66	14	14.85	0.94	3.528	3.32
304.34	8	12.39	0.65	3.528	2.29
313.84	9	12.56	0.72	3.528	2.54
323.31	2	9.84	0.20	3.528	0.71
332.81	5	10.64	0.47	3.528	1.66

^a From Table 3 and bulk density data.

Table 8. Accumulation rate (in m.y. increments) of fish teeth at Site 527.

Time Increment (m.y.)	Accumulation Rate (N/cm ² per 10 ³ y.)
47-48	0.31
48-49	0.64
49-50	0.76
51-52	0.20
52-53	0.73
53-54	2.37
54-55	1.75
55-56	3.51
56-57	5.5
57-58	1.7
58-59	2.4
59-60	2.7
60-61	1.6
61-62	1.8
62-63	2.47
63-64	1.2
64-65	1.5
65-66	0.35
66-66.46	1.01
66.46-67	3.1
67-68	2.7
68-69	1.2

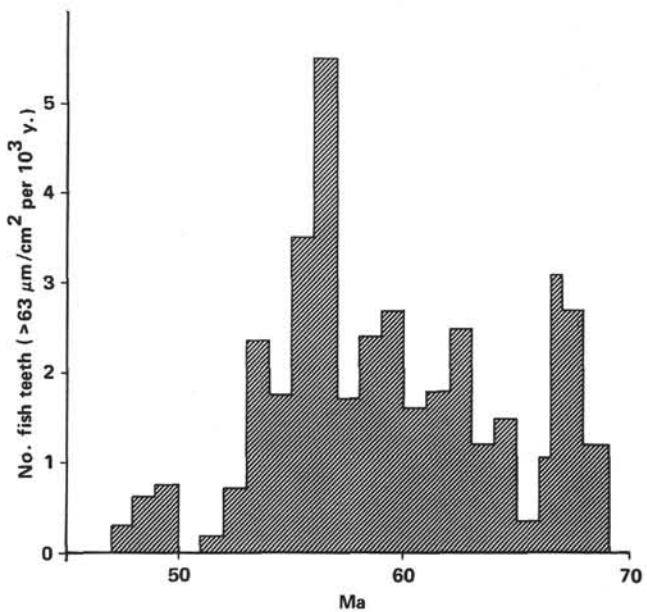


Figure 9. Accumulation of fish teeth (ichthyoliths) in the >63 μm fraction at Site 527. Data from Tables 7 and 8.

2.5 km depths) since the late Pliocene as well as in the Maestrichtian and Danian, when this site was at about 1 km depth.

Precise biostratigraphy is essential for the further development of chronostratigraphy. Without chronostratigraphy, the fascinating study of changes in the productivity and budget of the ocean are impossible, and this study shows what a dramatic story is to be found in the accumulation history of the oceans. It is very much to be hoped that further drilling cruises will be as well designed to tackle this topic as Leg 74 was.

ACKNOWLEDGMENTS

NJS is particularly grateful to Dr. Jan Backman, of Stockholm University, who was in Cambridge with the support of a Swedish Government postdoctoral fellowship during much of the time that this work was being undertaken, for much assistance in unravelling the intricacies of nannofossil biostratigraphy. Dr. Backman also kindly located a certain number of nannofossil datum levels in addition to those picked by the authors of this chapter; this in no way implies NJS's lack of confidence in his shipboard colleagues, but reflects the convenience of expertise close at hand and the fact that NJS had a large number of samples to hand for the purpose of isotope studies.

NJS is also grateful to the Natural Environment Research Council for support; to M. A. Hall, C. Solanki, and M. Tabeski for help in the laboratory; and to Dr. John Line for computing assistance.

This study owes a great deal to Captain Clark and the drilling crew of the *Glomar Challenger*, who achieved the objectives of the cruise so admirably. We also owe a debt of gratitude to the DSDP Ocean Palaeoenvironment Panel for ensuring that the original concept of the leg was maintained through the long gestation period. Several of us well remember Bill Ryan first producing the seismic traverse down the flank of the Walvis Ridge that became the banner which held Leg 74 alive.

REFERENCES

- Backman, J., 1980. Miocene-Pliocene calcareous nannofossils and sedimentation rates from the Hatton Rockall Basin, NE Atlantic Ocean. *Stockholm Contrib. Geol.*, 36:1-99.
- Backman, J., and Shackleton, N. J., 1981. Quantitative biochronology of calcareous plankton of the Pliocene and Early Pleistocene of the Pacific region. *Proc. IGCP Int. Workshop Pacific Neogene Biostratigraphy, Osaka, Japan*, pp. 110-112.

- Berggren, W. A., Kent, D., and van Couvering, J., in press, a. The geochronology of the Neogene. In Snelling, N. (Ed.), *Geochronology and the Geological Record*. Geol. Soc. London Spec. Publ.
- Berggren, W. A., Kent, D., and Flynn, J. T., in press, b. *Cenozoic Geochronology: 1982*. In Snelling, N. (Ed.), Geol. Soc. London Spec. Publ.
- Bukry, D., 1975. Coccolith and silicoflagellate stratigraphy, northwestern Pacific Ocean, Deep Sea Drilling Project, Leg 32. In Larson, R. L., Moberley, R. et al., *Init. Repts. DSDP*, 32: Washington (U.S. Govt. Printing Office), 677-701.
- Donnelly, T. W., 1982. Worldwide continental denudation and climatic deterioration during the late Tertiary: Evidence from deep-sea sediments. *Geology*, 10:451-454.
- Doyle, P. S., and Riedel, W. R., 1978. Cretaceous to Neogene ichthyoliths in a giant piston core from the central North Pacific. *Micropaleontology*, 25:337-364.
- Hardenbol, J., and Berggren, W. A., 1978. A new Paleogene time scale. *The Geologic Time Scale*. Am. Assoc. Pet. Geol., Stud. Geol., 6:213-234.
- Honjo, S., Spencer, D. W., and Farrington, J. W., 1982. Deep advective transport of lithogenic particles in Panama Basin. *Science*, 216:516-518.
- Kent, D., in press. The Cenozoic paleomagnetic timescale. In Snelling, N. (Ed.), *Geochronology and the Geochronological Record*. Geol. Soc. London Spec. Publ.
- Lowrie, W., and Alvarez, W., 1977. Upper Cretaceous-Paleocene magnetic stratigraphy at Gubbio, Italy. III. Upper Cretaceous magnetic stratigraphy. *Geol. Soc. Am. Bull.*, 88:374-377.
- Lowrie, W., Alvarez, W., Napoleone, G., Perch-Nielsen, K., Pre-moli-Silva, I., and Toumarkine, M., 1982. Paleogene magnetic stratigraphy in Umbrian pelagic carbonate rocks: The Contessa Section, Gubbio. *Geol. Soc. Am. Bull.*, 93:414-432.
- Martini, E., 1971. Standard Tertiary and Quaternary calcareous nanoplankton zonation. In Farinacci, A. (Ed.), *Proc. II Int. Conf. Planktonic Microfossils* (Vol. 2): Rome (Edizioni Tecnoscienza), 739-785.
- Ness, G., Levi, S., and Couch, R., 1980. Marine magnetic anomaly timescales for the Cenozoic and Cretaceous: A precis, critique and synthesis. *Rev. Geophys. Space Phys.*, 18:753-770.
- Poore, R. Z., Tauxe, L., Percival, S. F., LaBrecque, J. L., Wright, R., Petersen, N. P., Smith, C. C., Tucker, P., and Hsü, K. J., in press. Late Cretaceous-Cenozoic magnetostratigraphy and biostratigraphy correlations of the South Atlantic Ocean: DSDP Leg 73. In Hsü, K. J., LaBrecque, J. L., et al., *Init. Repts. DSDP*, 73: Washington (U.S. Govt. Printing Office).
- Roggenthin, W. M., and Napoleone, G., 1977. Upper Cretaceous-Paleocene magnetic stratigraphy at Gubbio, Italy. IV. Upper Maastrichtian to Paleocene magnetic stratigraphy. *Geol. Soc. Am. Bull.*, 88:378-382.
- Tauxe, L., Tucker, P. E., Petersen, N. P., and LaBrecque, J. L., in press. The magnetostratigraphy of Leg 73 sediments. In Hsü, K. J., LaBrecque, J. L., et al., *Init. Repts. DSDP* 73: Washington (U.S. Govt. Printing Office).
- van Andel, Tj. H., Heath, G. R., and Moore, T. C., 1975. *Cenozoic History and Paleoceanography of the Central Equatorial Pacific Ocean*. Geol. Soc. Am. Mem., 143.

APPENDIX A
Carbonate Percentages and Ages (estimated from the control points in Table 1), Leg 74

Sub-bottom Depth (m)	Age (Ma)	Carbonate (%)	Sub-bottom Depth (m)	Age (Ma)	Carbonate (%)	Sub-bottom Depth (m)	Age (Ma)	Carbonate (%)	Sub-bottom Depth (m)	Age (Ma)	Carbonate (%)
Hole 525A			Hole 525A (Cont.)			Hole 525A (Cont.)			Hole 525A (Cont.)		
0.09	0.018	94	149.35	13.259	95	280.01	46.828	98	456.58	66.734	68
0.61	0.125	95	153.11	13.436	93	281.51	47.204	96	460.11	67.051	45
1.59	0.325	96	154.73	13.512	96	281.75	47.264	91	461.48	67.176	47
2.11	0.431	96	155.31	13.539	95	283.01	47.580	95	465.00	67.496	66
3.09	0.631	97	157.06	13.654	96	283.25	47.640	94	466.08	67.595	68
3.21	0.656	96	158.15	13.781	94	284.51	47.976	82	467.58	67.731	65
3.91	0.799	96	159.65	13.956	93	284.75	48.044	93	468.16	67.784	61
5.41	1.105	96	162.53	14.292	93	286.47	48.531	97	469.07	67.867	69
6.91	1.412	97	165.94	14.690	98	286.90	48.653	97	469.44	67.900	70
7.99	1.632	96	166.79	14.789	96	288.94	49.232	95	470.68	68.013	72
9.49	1.925	96	168.29	14.964	95	290.44	49.657	97	472.31	68.162	70
10.99	2.126	96	169.80	15.141	97	291.94	50.040	97	473.93	68.309	71
12.61	2.343	95	174.73	15.637	95	293.44	50.246	96	475.43	68.441	68
14.11	2.544	95	176.23	15.748	93	294.94	50.453	98	476.93	68.550	71
15.61	2.745	97	177.54	15.845	97	297.94	50.865	97	478.26	68.641	66
17.55	3.005	97	179.01	15.954	94	298.23	50.905	97	488.16	69.324	60
19.05	3.128	96	179.04	15.956	96	299.73	51.112	99	489.77	69.433	42
22.00	3.230	96	180.51	16.065	94	301.23	51.318	97	491.25	69.528	31
23.50	3.283	96	180.54	16.067	97	302.73	51.524	96	492.75	69.624	43
24.36	3.313	97	181.93	16.170	96	304.23	51.731	99	493.90	69.698	44
26.10	3.373	97	182.46	16.209	98	305.73	51.937	98	494.40	69.730	55
27.60	3.426	97	183.95	16.319	97	307.72	52.211	96	497.58	69.934	41
29.10	3.478	96	184.12	16.332	94	309.22	52.417	98	497.71	69.942	31
30.96	3.543	96	184.81	16.383	94	310.72	52.613	99	499.20	70.038	28
31.61	3.565	95	186.31	16.494	92	312.22	52.723	93	500.66	70.132	36
33.11	3.630	98	187.81	16.605	95	313.72	52.834	99	502.21	70.231	41
35.06	3.745	99	188.01	16.620	90	315.22	52.944	97	503.71	70.328	51
36.56	3.834	96	189.05	16.697	90	316.72	53.055	98	507.23	70.553	43
38.06	3.923	97	189.31	16.716	95	317.43	53.107	97	508.86	70.658	22
39.56	4.012	99	190.55	16.808	95	318.93	53.217	97	510.15	70.741	39
41.07	4.101	97	190.81	16.827	92	320.43	53.328	95	511.78	70.846	10
42.57	4.190	96	192.05	16.919	92	321.93	53.439	98	513.17	70.935	36
43.18	4.226	96	192.47	16.950	93	323.43	53.549	96	514.76	71.037	31
44.68	4.314	98	193.97	17.128	91	324.93	53.660	97	516.69	71.161	21
46.18	4.403	97	194.31	17.181	94	326.43	53.770	96	518.16	71.255	14
47.58	4.486	96	195.47	17.362	92	326.93	53.807	96	520.03	71.375	10
51.95	4.725	96	196.36	17.500	92	328.43	53.917	98	521.31	71.457	28
53.45	4.807	96	197.31	17.611	95	331.43	54.322	98	522.68	71.545	60
54.95	4.888	96	197.76	17.628	92	334.43	54.837	94	527.16	71.833	61
56.35	4.965	94	198.81	17.666	96	335.93	55.094	99	528.09	71.893	42
57.85	5.030	99	199.26	17.683	92	336.43	55.179	99	529.18	71.962	64
59.35	5.082	100	200.31	17.721	94	337.93	55.300	98	530.92	72.074	63
60.75	5.131	97	201.17	17.752	95	339.43	55.408	99	535.99	72.400	38
62.25	5.183	95	201.81	17.776	96	345.78	55.867	90	537.49	72.496	61
65.14	5.284	95	202.67	17.807	92	351.68	56.124	99	538.68	72.572	41
66.64	5.337	99	203.10	17.823	92	353.18	56.137	99	548.48	73.201	30
68.14	5.389	98	204.10	17.859	92	354.68	56.150	100	561.31	74.025	64
69.55	5.438	97	204.17	17.862	94	355.25	56.155	98			
71.05	5.491	96	205.60	17.914	93	356.75	56.169	97			
72.55	5.543	93	206.56	17.949	92	358.25	56.182	97			
74.06	5.596	93	207.10	17.969	95	359.75	56.195	96			
75.56	5.648	97	208.06	18.028	96	361.25	56.208	97			
75.84	5.658	97	208.60	18.166	97	366.30	56.253	95			
78.41	5.747	96	209.56	18.411	95	367.80	56.266	93			
79.91	5.800	96	210.10	18.549	98	369.30	56.280	97			
81.41	5.852	97	211.60	18.932	96	370.80	56.293	97			
82.98	5.907	99	212.71	19.215	99	372.30	56.353	98			
87.25	6.056	96	214.21	19.598	99	374.21	56.417	89			
89.71	6.142	99	215.71	19.981	99	375.71	56.438	93			
91.66	6.210	95	217.21	20.364	96	377.21	56.458	97			
93.16	6.262	97	218.71	20.747	96	378.71	56.478	79			
94.66	6.315	97	222.21	21.641	95	380.21	56.498	97			
95.19	6.333	95	223.71	22.024	93	381.71	56.518	93			
96.69	6.386	96	225.21	22.407	95	383.71	56.544	95			
98.19	6.758	97	226.71	22.790	97	385.21	56.564	91			
99.21	7.092	99	228.21	22.848	98	386.71	56.584	94			
99.59	7.217	95	229.71	22.889	99	388.21	56.690	84			
101.09	7.709	96	231.21	22.934	98	389.71	57.099	95			
102.59	8.201	94	241.21	23.235	95	391.21	57.507	100			
103.99	8.564	94	242.71	23.280	99	392.71	57.757	92			
105.49	8.758	95	244.21	23.326	98	402.73	59.083	95			
109.34	9.258	94	245.71	23.371	99	404.21	59.228	97			
110.84	9.453	94	247.21	23.416	98	405.71	59.374	97			
112.25	9.636	96	248.71	23.461	98	407.21	59.521	93			
113.06	9.741	97	250.21	23.506	97	408.71	59.668	88			
114.56	9.935	96	250.71	23.521	96	410.21	59.814	87			
116.06	10.130	96	252.21	23.566	95	411.71	59.961	98			
117.69	10.342	93	253.71	23.611	94	412.21	60.010	79			
119.19	10.536	96	255.21	23.657	98	413.71	60.136	92			
120.69	10.679	96	256.71	23.704	97	415.21	60.228	94			
126.76	11.156	93	258.21	23.814	95	416.69	60.319	91			
128.26	11.273	93	259.71	23.923	97	421.69	60.760	75			
129.76	11.391	95	260.21	23.959	97	423.19	60.949	85			
131.85	11.555	93	261.71	24.069	94	423.19	61.803	91			
133.35	11.673	93	268.11	24.535	95	432.69	61.910	78			
134.85	11.790	96	269.71	24.652	96	434.19	62.056	84			
135.10	11.810	96	271.21	24.761	93	435.69	62.404	80			
136.60	11.928	96	272.68	24.868	95	441.61	63.779	82			
138.10	12.225	96	272.71	24.871	94	442.58	64.004	80			
139.30	12.691	95	274.18	24.978	93	444.09	64.362	67			
140.57	12.847	93	274.21	24.980	95	445.59	64.749	66			
142.07	12.917	94	275.71	25.089	97	447.21	65.198	53			
144.21	13.018	97	277.52	25.221	95	448.50	65.628	67			
145.71	13.088	94	278.02	25.258	95	452.71	66.516	57			
146.62	13.131	94	278.46	25.290	93	453.68	66.571	76			
148.97	13.241	96	278.65	40.720	96	455.12	66.652	76			

Appendix A. (Continued).

Sub-bottom Depth (m)	Age (Ma)	Carbonate (%)	Sub-bottom Depth (m)	Age (Ma)	Carbonate (%)	Sub-bottom Depth (m)	Age (Ma)	Carbonate (%)	Sub-bottom Depth (m)	Age (Ma)	Carbonate (%)
Hole 526A (Cont.)			Hole 526A (Cont.)			Hole 527 (Cont.)			Hole 528 (Cont.)		
82.10	10.893	96	218.91	37.273	94	184.64	56.478	96	26.39	2.885	93
83.60	11.111	98	219.53	37.318	94	187.64	56.688	94	27.87	3.101	97
85.10	11.328	97	220.41	37.381	97	189.66	56.829	95	29.06	3.133	94
85.51	11.388	96	221.03	37.426	96	191.16	56.934	89	29.33	3.140	92
87.01	11.605	97	222.53	37.535	95	199.19	57.495	90	30.83	3.181	95
88.51	11.823	99	223.03	37.571	93	200.61	57.594	76	32.35	3.222	96
88.90	11.880	96	224.03	37.643	95	202.11	57.699	90	33.83	3.262	95
91.40	12.298	95	224.53	37.679	95	203.61	57.804	94	35.24	3.300	95
92.90	12.566	98	226.19	37.799	96	208.71	58.160	94	36.74	3.341	94
94.13	12.786	98	227.53	37.896	97	210.21	58.265	94	38.23	3.381	95
95.63	12.891	98	229.03	38.005	100	218.11	58.817	92	38.27	3.382	95
97.13	12.986	98	230.53	38.113	99	219.61	58.922	93	39.73	3.422	96
98.63	13.082	97	232.53	38.258	100	221.25	59.078	92	41.23	3.463	96
99.16	13.116	97				227.71	59.727	91	42.61	3.500	95
100.66	13.211	96				229.07	59.863	89	44.11	3.541	96
102.16	13.307	98				230.57	60.014	91	45.61	3.581	95
103.06	13.365	98	0.46	0.062	88	232.16	60.173	88	47.01	3.643	94
104.56	13.460	97	1.96	0.266	95	237.20	60.679	86	48.51	3.733	96
106.06	13.556	98	3.46	0.470	97	238.60	60.825	74	50.01	3.824	94
107.33	13.740	95	4.96	0.673	94	240.21	61.002	85	52.78	3.991	95
108.83	14.102	97	6.46	0.877	93	241.72	61.167	90	54.28	4.082	97
110.35	14.468	94	7.71	1.046	93	243.18	61.327	88	55.78	5.010	98
111.33	14.704	99	9.47	1.285	90	244.63	61.485	88	57.46	5.134	93
113.43	15.211	98	15.40	2.041	96	246.92	61.736	88	58.74	5.229	96
114.93	15.723	96	18.64	2.367	96	248.42	61.900	90	60.17	5.335	93
116.11	16.599	95	20.14	2.584	94	249.74	62.044	83	61.67	5.446	97
117.61	17.618	97	21.64	2.820	95	256.20	62.751	82	63.17	5.558	93
119.14	17.786	96	23.14	3.056	93	257.70	62.915	82	64.91	5.687	99
121.73	21.391	98	24.64	3.149	96	259.20	63.144	82	69.96	6.061	94
123.23	22.826	98	28.15	3.291	96	260.70	63.522	81	70.70	6.116	96
124.73	22.857	98	29.65	3.352	95	261.31	63.601	76	73.83	6.348	96
125.08	22.865	96	37.72	3.678	98	275.05	65.707	60	75.33	6.459	94
126.58	22.896	99	39.22	3.739	96	276.55	65.941	48	76.83	6.571	94
128.08	22.928	98	40.72	3.800	96	278.05	66.174	30	78.10	6.665	95
129.35	22.954	100	47.15	4.060	95	279.64	66.407	71	79.60	6.776	97
130.85	22.986	98	48.65	4.141	97	281.14	66.508	66	81.10	6.887	93
132.35	23.017	97	50.15	4.264	97	282.64	66.572	64	82.31	6.977	90
134.14	23.055	97	51.65	4.388	97	284.63	66.656	69	87.91	7.392	94
135.24	23.078	97	53.15	4.511	97	286.13	66.720	75	91.19	7.635	98
136.74	23.110	95	54.65	4.634	98	287.63	66.782	85	92.69	7.747	97
138.13	23.139	97	56.91	4.820	98	289.13	66.844	88	94.19	7.858	97
139.63	23.170	95	59.60	5.039	97	294.85	67.081	78	95.50	7.955	96
141.13	23.202	96	66.61	5.584	95	306.81	67.576	76	97.00	8.066	95
142.55	23.232	97	68.11	5.700	94	297.85	67.205	86	98.50	8.177	96
142.63	23.233	98	69.61	5.817	97	299.35	67.267	78	100.90	8.355	90
144.33	23.269	98	71.11	5.934	97	300.85	67.329	81	105.60	9.455	94
145.83	23.300	99	72.61	6.050	97	302.35	67.391	78	107.10	9.975	94
147.22	23.330	95	73.67	6.133	98	303.81	67.452	82	108.60	10.496	95
148.72	23.361	96	76.67	6.366	96	305.31	67.514	71	108.96	10.613	96
150.22	23.393	95	89.89	7.394	93	306.81	67.576	76	110.46	10.939	93
151.63	23.422	96	94.61	7.761	84	308.31	67.638	69	111.96	11.265	93
153.13	23.454	96	96.11	7.877	77	309.81	67.700	83	113.01	11.493	90
154.63	23.485	95	97.61	7.994	82	313.61	67.857	82	113.11	11.515	93
156.02	23.515	95	99.11	8.111	83	315.11	67.919	72	114.51	11.820	96
157.52	23.546	94	100.61	8.227	86	316.61	67.981	86	116.01	12.228	90
159.02	23.578	95	104.21	8.930	69	318.11	68.043	80	117.78	12.889	91
160.43	23.751	96	105.71	10.869	52	319.61	68.105	67	118.49	13.590	76
161.93	24.419	94	107.21	11.219	56	320.58	68.146	80	122.25	16.637	85
163.43	25.087	94	108.71	11.570	38	322.64	68.231	83	126.21	16.781	92
164.83	25.710	98	110.21	11.921	21	324.43	68.305	71	127.71	16.836	92
166.33	26.377	96	111.71	12.270	23	325.93	68.367	81	128.55	16.867	91
167.83	27.045	96	113.21	18.078	24	327.35	68.426	43	131.61	16.978	83
170.30	28.116	95	113.60	28.306	39	328.75	68.484	72	136.11	17.708	74
171.80	28.353	94	115.10	34.845	23	330.32	68.549	69	141.05	17.867	78
173.91	28.687	96	116.60	35.136	27	331.69	68.605	69	144.05	17.963	94
175.41	28.925	94	118.10	35.428	39	332.89	68.655	66	145.55	18.214	89
176.91	29.162	94	119.60	35.719	18	334.16	68.707	59	147.05	19.156	88
177.69	29.285	96	121.10	36.010	78	336.03	68.785	54	148.55	20.098	91
179.19	29.523	95	122.60	36.302	87	336.97	68.824	66	150.05	20.613	87
180.69	29.760	95	123.11	36.401	89				150.64	20.715	82
182.43	30.036	95	124.61	36.692	92				152.14	20.975	89
183.93	30.273	96	133.09	40.964	13	0.11	0.012	88	153.64	21.265	87
185.43	30.629	93	134.59	41.787	36	0.34	0.038	93	155.14	21.632	82
187.04	31.026	97	136.09	42.609	16	1.61	0.182	91	156.64	21.999	96
188.54	31.397	92	137.59	45.184	50	1.85	0.209	90	158.14	22.365	71
190.04	31.768	95	139.09	47.625	81	3.08	0.348	90	159.64	22.732	89
195.81	33.193	97	142.20	48.307	89	3.11	0.351	92	160.51	22.945	90
197.31	33.564	96	145.20	49.350	89	4.58	0.517	89	162.01	23.312	89
198.81	33.934	95	146.70	49.864	92	4.61	0.521	89	163.51	23.678	91
200.61	34.379	96	148.20	50.372	91	6.08	0.687	89	165.01	24.045	89
201.11	34.502	96	152.41	51.605	88	6.11	0.690	91	166.51	24.412	86
203.61	35.120	95	153.91	52.138	91	7.58	0.856	90	168.01	24.779	91
204.03	35.224	93	155.41	52.775	92	7.60	0.858	91	169.51	25.145	87
204.54	35.350	96	156.91	53.116	94	7.66	0.865	91	170.11	25.292	88
205.53	35.594	94	161.81	54.229	93	9.16	1.034	90	171.61	25.655	91
206.04	35.720	95	162.68	54.427	96	10.66	1.204	94	174.61	26.371	90
207.03	35.965	95	164.18	54.732	94	12.04	1.360	93	175.11	26.491	87
207.54	36.091	94	165.68	54.891	98	12.16	1.373	91	177.61	27.088	89
208.53	36.336	96	167.18	55.050	90	13.54	1.496	92	179.37	27.508	91
210.03	36.631	95	168.68	55.209	98	15.04	1.594	95	180.87	27.866	92
211.53	36.740	95	170.47	55.399	94	17.76	1.773	93	182.37	28.265	87
212.8											

Appendix A. (Continued).

Sub-bottom Depth (m)	Age (Ma)	Carbonate (%)	Sub-bottom Depth (m)	Age (Ma)	Carbonate (%)	Sub-bottom Depth (m)	Age (Ma)	Carbonate (%)	Sub-bottom Depth (m)	Age (Ma)	Carbonate (%)		
Hole 528 (Cont.)													
194.85	31.912	89	404.08	65.975	10	81.03	22.188	94	211.34	42.289	90		
196.35	32.139	90	405.24	66.095	64	82.53	22.811	94	212.84	42.989	88		
197.85	32.367	88	407.02	66.461	52	84.03	11.843	93	214.34	43.689	90		
198.14	32.411	84	407.11	66.465	69	84.91	22.863	98	215.84	44.389	89		
199.64	32.639	89	408.61	66.531	71	86.41	22.896	89	217.34	45.089	89		
201.14	32.867	88	410.11	66.597	80	87.91	22.928	97	219.34	46.022	88		
202.64	33.049	89	411.61	66.664	81	95.39	23.092	94	220.84	46.722	91		
207.66	33.636	85	413.11	66.730	84	96.89	23.125	95	222.34	47.422	89		
209.16	33.811	90	417.01	66.931	61	98.39	23.158	96	223.84	47.993	91		
210.66	33.986	89	418.51	67.008	68	99.89	23.191	97	225.34	48.414	93		
226.61	36.492	86	420.01	67.086	75	101.39	23.224	97	236.58	51.797	84		
228.16	37.000	81	421.51	67.164	71	102.89	23.257	94	238.08	52.280	97		
236.76	37.737	81	423.01	67.242	81	104.81	23.299	93	239.58	52.763	95		
237.60	37.875	86	424.51	67.320	70	109.31	23.397	92	241.08	53.246	95		
246.34	44.472	83	426.60	67.428	76	110.81	23.430	95	242.58	53.729	96		
247.84	45.604	85	428.39	67.521	85	112.31	23.463	94	244.08	54.212	97		
249.59	46.502	89	436.02	67.918	87	113.41	23.487	94	246.05	54.846	93		
250.81	46.907	91	437.52	67.995	78	114.91	23.520	92	247.55	55.228	92		
252.16	47.355	90	438.52	68.047	78	116.41	23.553	95	249.05	55.331	96		
253.18	47.694	91	454.70	68.888	77	117.91	23.586	94	250.55	55.435	96		
255.33	48.290	93	456.61	68.987	57	119.41	23.797	95	252.05	55.539	95		
256.62	48.635	93	458.30	69.074	63	120.91	24.142	94	253.55	55.643	97		
258.12	50.180	94	459.61	69.142	74	124.41	24.945	92	255.05	55.746	98		
259.76	51.278	94	461.06	69.218	66	125.91	25.290	92	260.01	56.089	97		
261.22	52.179	93	466.21	69.485	52	127.41	25.634	94	261.51	56.193	97		
263.12	52.653	91	467.71	69.563	42	128.91	25.979	92	263.01	56.297	96		
266.31	53.327	92	469.42	69.652	67	130.41	26.323	93	265.17	56.599	95		
267.81	53.643	95	473.85	69.882	62	132.41	26.782	92	266.67	57.045	96		
269.31	53.960	93				133.91	27.127	95	268.17	57.490	95		
274.31	54.377	92	Hole 529										
275.81	54.495	93	0.97	0.257	92	135.41	27.471	95	284.31	59.293	90		
277.31	54.613	94	2.47	0.522	96	136.91	27.815	94	293.91	59.548	91		
278.81	54.730	91	3.97	0.661	96	138.41	28.169	93	295.10	59.579	86		
285.16	55.218	94	5.47	0.800	97	142.25	29.272	96	296.69	59.621	86		
286.66	55.293	91	6.97	0.940	96	143.41	29.501	96	298.07	59.658	88		
293.35	55.626	95	8.86	1.116	96	144.91	29.901	95	299.57	59.698	84		
294.85	55.701	96	10.36	1.255	96	146.41	30.300	93	303.05	59.790	91		
296.35	55.776	92	11.86	1.394	94	148.41	31.100	94	304.58	59.830	86		
297.85	55.851	97	13.36	1.534	94	150.91	31.499	97	306.08	59.870	86		
299.35	55.926	96	14.86	1.673	96	154.18	32.370	91	307.58	59.910	76		
303.14	56.114	97	16.36	1.813	96	155.68	32.770	94	312.57	60.042	89		
304.64	56.189	94	17.86	2.284	93	157.18	33.169	93	314.07	60.082	90		
306.14	56.264	94	18.36	2.627	94	158.68	33.569	95	315.57	60.165	91		
307.64	56.350	97	19.86	3.123	93	160.18	33.969	93	317.07	60.284	86		
309.14	56.447	92	21.36	3.167	96	162.18	34.102	93	322.03	60.634	86		
310.64	56.544	93	22.86	3.210	97	163.68	34.624	96	323.53	60.725	79		
312.14	56.976	91	27.62	3.348	97	165.18	34.656	94	325.03	60.865	82		
313.64	57.629	86	29.12	3.391	96	166.68	34.688	95	332.21	61.607	85		
315.14	57.727	90	30.62	3.434	97	168.18	34.720	93	333.71	61.643	85		
316.64	57.824	96	32.12	3.478	95	170.31	34.765	90	335.21	61.679	86		
321.75	58.158	92	33.62	3.521	97	171.81	34.797	95	336.71	61.715	85		
324.75	58.353	90	36.62	3.723	97	173.31	34.829	94	338.10	61.748	87		
326.25	58.451	91	37.11	3.945	98	174.81	34.861	92	341.42	61.827	88		
331.35	58.784	91	47.16	14.100	95	176.31	34.893	91	342.92	61.862	84		
332.85	58.881	94	48.65	14.358	98	177.81	34.924	95	351.01	62.278	86		
334.35	59.035	92	50.16	14.619	95	179.31	34.956	93	352.51	62.458	86		
335.85	59.274	89	51.66	14.879	97	179.86	34.968	94	360.12	63.374	72		
340.78	60.058	94	53.16	15.138	92	181.31	34.999	89	361.62	63.555	79		
342.28	60.297	85	54.66	15.398	94	182.86	35.032	90	369.70	64.527	74		
351.20	61.136	87	56.16	16.657	96	184.36	35.064	90	371.20	64.707	72		
359.59	61.391	75	56.71	17.013	92	185.86	35.096	92	372.70	64.888	74		
361.09	61.436	84	58.21	17.080	94	187.36	35.269	92	379.11	65.483	55		
362.59	61.482	86	59.71	17.148	90	188.86	35.466	94	380.72	65.631	75		
369.17	61.681	91	61.21	17.216	92	190.25	35.648	95	382.62	65.807	47		
370.67	61.726	87	62.71	17.283	93	191.75	35.845	95	383.71	65.911	68		
371.48	61.751	89	64.21	17.351	96	193.25	36.042	95	385.56	66.161	10		
378.55	61.965	79	65.53	17.411	98	194.75	36.239	94	387.54	66.429	63		
380.05	62.032	84	67.03	17.478	95	196.25	36.433	95	388.68	66.583	70		
381.55	62.170	85	68.53	17.546	92	197.79	36.638	91	390.52	66.832	63		
382.05	62.216	81	70.03	17.628	92	198.84	36.775	95	392.52	67.103	84		
388.09	62.770	77	71.53	17.767	92	200.34	37.157	90	393.09	67.180	61		
389.68	62.916	77	74.53	18.288	96	201.84	37.857	89	394.71	67.399	63		
391.10	63.046	64	75.03	18.588	94	203.34	38.556	92	398.11	67.859	75		
392.80	63.700	69	76.53	19.488	93	204.84	39.256	92	399.61	68.062	77		
397.74	65.199	62	78.03	20.388	95	206.34	39.956	89	401.11	68.264	75		
399.34	65.470	71	78.03	20.884	95	208.34	40.890	95	402.61	68.467	70		
400.65	65.622	9	79.53	21.288	92	209.84	41.589	94					

APPENDIX B
Percentage of Sediment >63 µm at Leg 74 Sites^a

Sub-bottom Depth (m)	Age (Ma) ^b	Sediment (%)	Sub-bottom Depth (m)	Age (Ma) ^b	Sediment (%)	Sub-bottom Depth (m)	Age (Ma) ^b	Sediment (%)	Sub-bottom Depth (m)	Age (Ma) ^b	Sediment (%)
Site 525			Site 525 (Cont.)			Site 525 (Cont.)			Site 525 (Cont.)		
0.06	0.012	42.6	63.40	5.223	10.1	142.61	12.942	18.7	281.10	47.101	2.7
3.50	0.715	49.1	66.71	5.339	14.5	142.81	12.952	22.0	281.72	47.256	3.4
6.61	1.350	40.1	66.81	5.342	13.0	143.01	12.961	22.0	281.74	47.261	4.3
6.81	1.391	54.9	66.91	5.346	14.4	143.21	12.971	16.0	281.92	47.306	3.6
7.01	1.432	42.8	66.91	5.346	10.8	143.30	12.975	15.8	282.11	47.354	3.1
7.21	1.473	35.2	67.11	5.353	14.0	146.60	13.130	17.8	282.21	47.379	3.9
7.41	1.514	45.1	67.51	5.367	15.7	149.56	13.269	11.7	282.51	47.454	2.8
7.61	1.555	48.6	67.71	5.374	27.6	151.12	13.342	9.6	282.60	47.477	2.8
7.81	1.596	49.3	67.91	5.381	14.1	154.97	13.523	11.2	282.91	47.554	2.9
7.90	1.614	45.2	68.21	5.391	11.2	156.20	13.581	13.8	283.10	47.602	2.6
12.00	2.262	19.2	68.61	5.405	14.6	157.91	13.753	13.6	283.32	47.657	4.0
15.20	2.690	43.6	68.81	5.412	13.0	159.41	13.928	12.0	283.32	47.657	6.3
16.70	2.891	33.9	69.01	5.419	10.9	159.41	13.928	14.5	283.66	47.742	5.6
17.41	2.986	24.6	69.21	5.426	11.2	160.00	13.997	6.1	284.00	47.831	4.1
17.61	3.013	24.8	69.41	5.433	2.4	160.11	14.010	3.9	284.10	47.860	3.4
17.81	3.040	13.2	69.50	5.436	9.4	162.21	14.255	12.8	284.38	47.939	3.6
18.51	3.109	27.6	70.21	5.461	11.2	162.31	14.266	10.0	284.56	47.990	3.5
18.71	3.116	26.3	70.41	5.468	11.2	163.81	14.441	11.6	284.97	48.106	3.5
18.91	3.123	21.9	70.61	5.475	10.3	164.90	14.569	14.0	285.00	48.115	3.7
19.11	3.130	17.0	71.11	5.493	9.4	166.61	14.768	12.9	287.10	48.710	3.9
19.31	3.137	25.6	71.31	5.500	12.3	169.80	15.141	10.9	287.30	48.767	4.1
19.51	3.144	22.2	71.51	5.507	12.5	169.90	15.152	11.3	289.01	49.252	3.5
19.80	3.154	23.1	71.71	5.514	10.9	171.20	15.304	6.4	290.51	49.677	2.4
22.20	3.237	46.4	71.91	5.521	7.2	171.60	15.351	10.2	292.01	50.050	1.6
22.40	3.244	30.0	72.11	5.528	8.2	174.61	15.628	19.3	293.50	50.255	2.7
22.71	3.255	40.2	72.31	5.535	3.9	174.71	15.635	15.0	295.01	50.462	9.1
22.91	3.262	29.7	72.61	5.545	10.2	174.71	15.635	15.0	298.00	50.874	4.7
23.11	3.269	22.9	72.81	5.552	9.9	174.91	15.650	15.3	298.10	50.887	5.4
23.31	3.276	22.3	73.01	5.559	9.8	174.91	15.650	15.3	301.19	51.312	4.7
23.51	3.283	19.3	74.11	5.597	12.6	175.11	15.665	16.0	301.29	51.326	3.8
23.71	3.290	23.7	74.31	5.604	11.5	175.31	15.680	18.0	301.39	51.340	5.2
23.91	3.297	21.3	74.73	5.619	12.3	175.31	15.680	18.0	301.49	51.354	4.1
24.21	3.307	24.2	74.94	5.626	14.4	175.51	15.695	23.6	301.59	51.367	3.2
24.41	3.314	17.8	75.14	5.633	6.8	175.51	15.695	18.0	301.69	51.381	3.9
24.60	3.321	22.8	75.41	5.643	32.7	175.81	15.717	31.3	301.79	51.395	3.6
26.61	3.391	15.2	75.61	5.650	11.3	175.81	15.717	31.4	301.99	51.422	3.3
26.81	3.398	18.9	75.81	5.657	11.3	176.01	15.732	18.0	302.09	51.436	3.6
27.11	3.409	25.9	75.90	5.660	8.5	176.01	15.732	18.1	302.19	51.450	3.0
27.31	3.416	25.9	79.71	5.793	9.6	176.21	15.746	18.0	302.29	51.464	3.0
27.51	3.423	16.2	81.01	5.838	10.2	176.21	15.746	14.4	302.39	51.477	2.8
27.71	3.429	28.6	82.30	5.883	10.1	176.41	15.761	13.3	307.50	52.180	2.9
27.91	3.436	20.7	82.40	5.887	7.9	176.41	15.761	13.3	317.10	53.083	2.1
28.11	3.443	38.1	82.88	5.904	7.7	176.80	15.790	11.6	322.79	53.502	10.1
28.31	3.450	22.9	87.90	6.079	10.2	177.01	15.806	23.3	326.60	53.783	3.8
28.61	3.461	24.0	88.01	6.083	9.5	182.40	16.204	11.6	336.10	54.468	1.4
28.81	3.468	23.8	90.60	6.173	6.9	184.00	16.323	15.3	337.85	54.604	5.3
29.01	3.475	20.9	94.31	6.303	10.0	188.51	16.657	12.6	340.30	54.801	1.4
29.60	3.495	15.7	96.21	6.369	14.6	188.71	16.671	8.9	345.70	55.235	6.4
32.31	3.590	27.4	96.38	6.375	4.8	189.11	16.701	12.6	354.07	55.670	5.7
32.51	3.597	26.0	96.70	6.386	10.2	189.31	16.716	10.8	355.10	55.704	4.7
32.71	3.607	19.2	97.71	6.600	4.0	189.51	16.731	12.3	358.19	55.808	3.4
33.01	3.624	21.0	99.20	7.089	8.7	189.91	16.760	12.9	358.29	55.811	3.3
33.50	3.653	20.8	99.21	7.092	5.2	190.11	16.775	15.5	358.39	55.814	3.1
33.81	3.672	25.6	100.99	7.676	14.4	190.31	16.790	12.3	358.49	55.818	3.8
35.91	3.796	19.0	101.18	7.739	14.6	190.61	16.812	9.9	358.59	55.821	3.7
36.11	3.808	15.8	102.00	8.008	13.8	190.81	16.827	11.2	358.69	55.824	6.1
36.31	3.819	23.8	102.11	8.044	21.1	191.01	16.842	12.3	358.79	55.828	3.8
36.51	3.831	15.8	102.17	8.064	17.2	191.21	16.856	13.1	358.89	55.831	4.0
36.71	3.843	15.0	103.40	8.467	16.0	191.41	16.871	13.2	358.99	55.834	4.0
36.91	3.855	19.9	105.01	8.696	24.0	191.61	16.886	12.9	359.09	55.838	4.0
37.11	3.867	25.3	106.10	8.837	9.3	191.80	16.900	11.7	359.19	55.841	4.2
37.41	3.884	17.7	106.21	8.852	12.4	192.31	16.938	10.6	359.29	55.844	4.4
37.61	3.896	17.3	106.40	8.876	16.0	192.51	16.953	11.5	359.39	55.848	5.3
37.81	3.908	22.3	112.50	9.668	15.5	192.71	16.967	12.4	359.49	55.851	3.4
38.01	3.920	17.1	113.61	9.812	17.2	192.91	16.982	13.1	359.59	55.854	3.8
38.21	3.932	14.5	113.81	9.838	12.5	193.11	16.997	13.7	361.80	55.928	4.5
38.60	3.955	24.8	115.11	10.007	23.1	193.41	17.041	16.3	367.07	56.105	6.3
38.81	3.967	19.5	116.81	10.228	18.3	193.50	17.055	9.7	371.57	56.255	7.5
39.01	3.979	16.2	116.90	10.239	15.8	193.61	17.072	17.6	372.80	56.297	6.8
39.81	4.026	19.5	112.61	10.830	13.6	193.81	17.103	13.7	376.57	56.642	7.8
40.31	4.056	16.8	123.91	10.932	18.5	194.01	17.134	13.8	382.09	57.156	7.5
40.51	4.068	14.1	124.11	10.948	17.7	194.21	17.165	13.0	383.50	57.288	9.8
40.71	4.080	14.2	124.60	10.986	24.4	194.41	17.196	13.0	390.09	57.902	3.8
41.51	4.127	11.2	128.51	11.293	17.7	194.61	17.228	15.0	393.10	58.182	5.9
41.81	4.145	20.6	129.36	11.360	14.0	194.91	17.274	13.3	404.59	59.265	6.2
42.01	4.156	17.5	130.10	11.418	15.1	195.11	17.305	13.0	409.09	59.705	8.5
42.21	4.168	15.1	132.61	11.615	23.2	195.51	17.368	13.7	412.10	59.999	7.5
42.41	4.180	13.7	132.71	11.623	22.3	195.71	17.399	13.7	414.71	60.197	6.9
42.61	4.192	14.9	134.50	11.763	17.0	195.91	17.430	14.7	417.20	60.350	16.1
42.90	4.209	10.0	134.66	11.776	15.0	196.20	17.475	12.1	423.21	60.952	5.2
44.41	4.298	5.0	134.82	11.788	15.0	200.60	17.732	9.6	423.50	60.988	7.7
45.91	4.387	5.5	137.20	11.975	13.2	203.00	17.819	13.9	433.72	61.984	4.7
46.61	4.428	7.4	138.30	12.303	12.9	205.00	17.892	10.5	436.10	62.499	11.9
47.41	4.476	2.6	139.18	12.645	13.2	209.40	18.370	8.3	442.50	63.986	27.3
47.60	4.487	13.3	139.41	12.734	13.3	212.50	19.162	7.7	442.70	64.032	21.4
47.60	4.487	14.1	139.61	12.801	10.8	219.70	21.000	7.7	442.77	64.048	0.7
48.30	4.526										

Appendix B. (Continued).

Sub-bottom Depth (m)	Age (Ma) ^b	Sediment (%)	Sub-bottom Depth (m)	Age (Ma) ^b	Sediment (%)	Sub-bottom Depth (m)	Age (Ma) ^b	Sediment (%)	Sub-bottom Depth (m)	Age (Ma) ^b	Sediment (%)
Site 525 (Cont.)			Site 526 (Cont.)			Site 526 (Cont.)			Site 526 (Cont.)		
449.90	65.933	28.3	31.41	4.137	61.2	52.11	5.831	57.4	72.21	9.246	26.5
451.65	66.436	32.7	31.49	4.144	52.5	52.20	5.847	45.2	72.41	9.281	29.9
451.73	66.461	20.0	31.60	4.154	58.9	52.21	5.848	48.7	72.61	9.315	29.7
451.86	66.468	22.9	31.71	4.164	66.9	52.40	5.881	46.4	72.81	9.350	37.1
452.48	66.503	4.4	31.81	4.173	50.0	52.41	5.882	46.4	73.01	9.384	29.8
453.13	66.540	3.8	32.01	4.191	55.4	52.60	5.914	49.4	73.21	9.418	23.6
454.90	66.639	9.1	32.11	4.200	52.6	52.61	5.916	49.4	73.41	9.453	18.5
456.98	66.766	9.2	32.20	4.208	62.7	52.80	5.948	16.7	73.61	9.487	58.5
457.50	66.814	7.0	33.05	4.284	46.5	52.81	5.950	16.7	73.85	9.529	23.6
462.30	67.251	6.1	33.66	4.339	75.3	53.10	5.999	43.7	74.01	9.556	57.7
466.55	67.637	9.1	34.55	4.419	64.9	53.11	6.001	43.7	74.08	9.568	52.2
470.91	68.034	4.4	36.05	4.526	78.2	53.30	6.033	28.6	74.38	9.620	54.5
475.84	68.471	4.1	38.02	4.609	43.1	53.31	6.035	28.6	74.51	9.642	22.8
478.50	68.658	20.1	39.52	4.673	41.8	53.50	6.067	34.3	74.71	9.676	58.4
497.60	69.935	60.6	41.02	4.737	59.2	53.51	6.068	34.3	75.11	9.745	46.9
			41.31	4.749	54.4	53.70	6.101	24.9	75.29	9.776	50.5
Site 526			41.42	4.754	57.1	53.71	6.102	24.9	75.48	9.809	58.4
0.71	0.099	91.5	41.52	4.758	51.9	53.90	6.134	40.0	75.51	9.814	64.3
1.94	0.270	89.0	41.91	4.775	54.0	53.91	6.136	40.0	75.68	9.843	54.5
3.10	0.432	69.7	42.10	4.783	51.5	54.10	6.168	50.8	75.90	9.881	54.7
3.14	0.437	58.3	42.31	4.792	45.1	54.11	6.170	50.8	76.71	10.020	54.1
3.19	0.444	60.8	42.51	4.800	41.0	54.31	6.202	34.1	77.61	10.175	59.7
3.25	0.452	56.9	42.66	4.807	49.3	56.03	6.495	15.1	78.21	10.278	56.9
3.30	0.458	61.3	43.39	4.838	55.3	56.20	6.524	35.4	78.41	10.313	55.4
3.38	0.467	40.1	44.31	4.877	37.5	56.40	6.558	47.8	78.61	10.347	55.5
3.50	0.480	71.0	44.42	4.882	51.4	56.60	6.592	48.7	78.81	10.382	67.5
7.10	0.883	71.1	44.50	4.885	42.9	56.82	6.629	42.0	79.21	10.450	51.0
15.71	1.845	78.6	44.70	4.894	50.7	57.00	6.659	37.0	79.41	10.485	56.5
15.91	1.868	76.6	44.90	4.902	55.5	57.26	6.703	38.1	79.61	10.519	62.2
16.11	1.890	70.5	44.89	4.902	44.4	57.53	6.749	37.0	79.81	10.554	66.9
16.20	1.900	67.6	45.10	4.911	50.7	57.70	6.778	39.4	80.01	10.588	57.6
16.31	1.914	76.0	45.30	4.919	46.0	57.90	6.812	55.2	82.41	10.938	64.2
16.91	1.991	76.3	45.50	4.928	39.6	58.10	6.846	42.2	83.01	11.025	55.8
17.11	2.016	69.4	45.62	4.933	32.5	58.30	6.880	34.0	83.21	11.054	57.3
17.31	2.042	64.3	46.39	4.966	59.6	58.50	6.913	33.5	83.41	11.083	58.3
17.51	2.067	64.0	46.51	4.971	51.4	58.70	6.947	41.2	83.61	11.112	51.0
17.70	2.092	76.6	46.61	4.975	57.9	58.85	6.973	51.5	83.81	11.141	54.6
17.71	2.093	83.3	46.71	4.979	61.3	60.40	7.235	52.4	84.21	11.199	52.9
17.93	2.121	82.9	46.80	4.983	24.6	60.60	7.269	41.4	84.41	11.228	49.0
18.11	2.144	74.3	47.00	4.991	50.0	60.80	7.303	51.3	84.61	11.257	51.6
18.31	2.170	50.3	47.07	4.994	49.4	61.00	7.337	48.0	85.01	11.315	45.9
18.51	2.195	74.5	47.14	4.997	54.5	61.20	7.371	28.0	85.57	11.396	54.0
18.71	2.221	68.2	47.31	5.019	38.4	61.40	7.404	51.9	87.07	11.614	51.0
18.88	2.243	65.8	47.40	5.034	42.9	61.60	7.438	47.2	88.57	11.832	47.4
20.71	2.476	80.4	47.52	5.054	48.4	61.66	7.448	48.5	90.01	12.050	58.7
20.75	2.482	65.5	47.57	5.063	42.5	61.76	7.465	54.0	90.21	12.086	54.3
20.91	2.502	63.2	47.71	5.086	37.5	61.90	7.489	66.3	91.61	12.336	55.9
21.11	2.528	77.6	47.80	5.102	36.1	62.10	7.523	46.9	93.21	12.621	54.4
21.31	2.553	75.2	47.89	5.117	55.9	62.30	7.557	44.1	95.31	12.870	49.7
21.71	2.604	74.7	47.91	5.120	41.5	62.50	7.591	44.3	95.61	12.889	63.6
21.91	2.630	70.1	48.00	5.135	37.1	62.70	7.625	44.7	95.81	12.902	62.3
22.25	2.673	58.4	48.11	5.154	38.7	62.90	7.658	52.3	96.01	12.915	49.1
22.31	2.681	69.7	48.20	5.169	39.3	63.10	7.692	57.0	96.21	12.928	58.4
24.01	2.898	62.6	48.40	5.203	40.2	63.16	7.702	50.4	96.41	12.940	41.2
24.26	2.930	58.9	48.64	5.244	41.4	63.26	7.719	49.8	96.61	12.953	49.6
24.31	2.937	62.7	48.70	5.254	21.3	63.40	7.743	51.5	96.81	12.966	55.8
24.91	3.013	71.0	48.81	5.273	52.2	63.41	7.745	58.2	97.11	12.985	56.2
25.11	3.039	66.6	48.90	5.288	33.5	63.41	7.745	58.2	97.31	12.998	52.0
25.31	3.064	73.4	49.01	5.306	41.3	63.60	7.777	28.8	97.51	13.011	54.8
25.51	3.090	74.9	49.07	5.317	21.6	63.60	7.777	49.1	97.71	13.023	58.4
25.71	3.116	72.7	49.22	5.342	42.8	63.61	7.779	49.1	98.11	13.049	60.8
25.76	3.122	67.9	49.30	5.356	39.9	63.80	7.811	60.0	98.49	13.073	56.3
25.91	3.141	75.0	49.39	5.371	52.2	63.81	7.813	60.0	98.71	13.087	55.0
26.11	3.167	78.7	49.41	5.374	48.8	64.00	7.845	59.7	98.91	13.100	53.0
26.31	3.192	65.0	49.50	5.389	32.6	64.01	7.846	59.7	99.11	13.113	45.5
26.51	3.218	63.3	49.61	5.408	41.3	64.20	7.879	62.7	99.31	13.125	56.0
26.71	3.243	65.0	49.70	5.423	47.5	64.21	7.880	62.7	99.51	13.138	60.5
26.91	3.269	57.9	49.81	5.442	46.9	64.40	7.912	65.7	99.81	13.157	66.2
27.11	3.295	52.6	49.90	5.457	49.0	64.41	7.914	65.7	100.11	13.176	62.5
27.26	3.314	51.8	49.99	5.472	54.4	64.60	7.946	60.4	100.31	13.189	49.5
27.31	3.320	54.5	50.01	5.476	32.9	64.80	7.980	57.9	100.71	13.215	60.0
27.51	3.346	59.0	50.11	5.493	30.6	64.80	7.980	57.9	101.11	13.240	47.6
27.71	3.371	52.6	50.21	5.510	34.2	65.00	8.014	53.1	101.61	13.272	57.7
27.91	3.397	52.8	50.31	5.527	25.4	65.01	8.016	63.7	101.91	13.291	46.1
28.11	3.422	58.2	50.41	5.544	31.1	65.01	8.016	53.1	103.00	13.361	48.2
28.81	3.512	61.1	50.51	5.560	31.5	65.20	8.048	58.3	103.01	13.361	48.2
28.91	3.525	65.9	50.71	5.594	20.8	65.21	8.050	58.3	103.21	13.374	55.3
29.01	3.537	63.0	50.81	5.611	32.8	65.40	8.082	57.1	103.20	13.374	55.3
29.11	3.550	58.3	50.91	5.628	35.6	65.41	8.083	57.1	103.40	13.386	55.6
29.20	3.562	59.2	51.01	5.645	44.0	65.60	8.116	62.4	103.41	13.387	53.5
29.36	3.582	59.8	51.11	5.662	39.3	65.61	8.117	62.4	103.60	13.399	49.3
29.71	3.670	64.0	51.21	5.679	42.8	65.81	8.151	55.8	103.80	13.412	49.5
29.79	3.697	64.0	51.31	5.696	36.5	66.00	8.183	57.5	103.81	13.412	49.5
29.90	3.733	62.7	51.41	5.713	46.5	66.01	8.185	57.5	104.01	13.425	53.9
29.99	3.763	57.2	51.51	5.730	50.0	66.15	8.209	56.1	104.00	13.425	53.9
30.10	3.800	68.6	51.61	5.747	16.5	66.16	8.210	56.1	104.20	13.437	55.7
30.20	3.833	61.0	51.61	5.747	18.4	66.30	8.234	46.5	104.21	13.438	55.7
30.31	3.870	56.0	51.61	5.747	18.4	66.30	8.234	46.5	104.50	13.456	45.5

Appendix B. (Continued).

Sub-bottom Depth (m)	Age (Ma) ^b	Sediment (%)	Sub-bottom Depth (m)	Age (Ma) ^b	Sediment (%)	Sub-bottom Depth (m)	Age (Ma) ^b	Sediment (%)	Sub-bottom Depth (m)	Age (Ma) ^b	Sediment (%)
Site 526 (Cont.)			Site 526 (Cont.)			Site 527 (Cont.)			Site 527 (Cont.)		
105.30	13.507	44.6	177.71	29.289	8.1	148.27	50.393	0.6	273.82	65.516	4.2
105.31	13.508	44.6	177.80	29.303	8.2	152.26	51.561	0.5	274.01	65.545	5.7
105.50	13.520	54.9	178.81	29.463	2.8	152.28	51.567	0.6	274.20	65.575	6.2
105.51	13.521	54.9	180.11	29.668	12.0	152.56	51.648	0.8	274.41	65.607	6.3
105.70	13.533	55.3	180.50	29.730	2.8	153.60	51.956	1.2	275.14	65.721	0.6
105.71	13.534	55.3	180.71	29.763	3.2	153.70	52.015	0.3	275.15	65.723	11.8
106.00	13.552	49.2	180.80	29.778	3.6	153.78	52.062	0.8	275.25	65.738	1.4
106.01	13.553	49.2	182.20	29.999	3.7	153.80	52.073	1.5	275.28	65.743	4.8
106.20	13.565	50.1	183.20	30.158	4.3	156.78	53.086	2.5	275.32	65.749	4.7
106.21	13.566	50.1	184.20	30.318	4.8	161.50	54.159	2.6	275.36	65.756	1.5
106.40	13.578	55.2	185.19	30.494	2.8	163.07	54.516	3.8	275.52	65.780	1.4
106.41	13.578	55.2	186.20	30.674	4.7	167.50	55.084	4.6	275.71	65.810	0.6
106.60	13.590	63.6	187.46	30.899	3.9	168.91	55.234	2.9	276.07	65.866	14.6
106.61	13.591	63.6	188.70	31.119	3.7	170.50	55.402	6.6	276.21	65.888	6.6
106.80	13.612	61.3	188.96	31.166	6.3	171.70	55.530	6.9	276.21	65.888	8.1
106.81	14.614	61.3	190.46	31.433	4.8	172.29	55.592	4.0	276.28	65.899	9.3
107.81	13.856	66.9	193.69	32.008	3.9	175.65	55.850	5.3	276.49	65.932	5.6
109.31	14.217	53.7	196.00	32.420	5.5	180.17	56.166	3.5	276.55	65.941	11.7
110.81	14.579	62.3	199.00	32.954	3.7	180.40	56.182	3.0	276.74	65.971	14.3
111.91	14.844	41.4	200.40	33.204	6.2	184.71	56.483	9.0	276.92	65.999	16.1
112.01	14.868	50.6	201.90	33.471	7.9	185.90	56.566	6.7	277.11	66.028	19.1
112.21	14.916	50.5	203.38	33.735	8.6	189.85	56.842	6.5	277.22	66.045	10.3
112.41	14.965	54.3	204.76	33.981	11.4	199.81	57.538	3.5	277.42	66.076	7.4
112.61	15.013	59.4	206.26	34.248	6.3	202.24	57.708	2.7	277.73	66.125	8.2
112.81	15.061	52.6	211.00	35.092	7.6	204.31	57.853	2.2	277.94	66.158	12.6
113.01	15.109	57.9	213.21	35.486	7.7	210.50	58.285	2.6	278.28	66.208	5.4
113.41	15.206	48.9	214.71	35.753	12.7	218.14	58.819	8.0	278.35	66.218	3.3
113.51	15.230	49.0	216.21	36.020	9.1	218.30	58.830	1.5	278.81	66.286	3.4
113.81	15.302	48.7	217.71	36.288	7.7	218.34	58.833	4.9	279.06	66.322	11.2
114.01	15.351	56.6	219.21	36.555	18.8	218.63	58.853	3.5	279.28	66.355	12.5
113.21	15.399	50.0	220.71	36.822	35.8	219.38	58.906	7.6	279.45	66.379	8.2
114.41	15.447	49.2				219.72	58.930	7.4	279.48	66.384	4.7
114.71	15.559	55.5				219.89	58.942	5.9	279.65	66.409	18.7
114.91	15.708	56.7				220.21	58.974	1.6	279.72	66.419	10.1
115.01	15.782	58.3	3.38	0.310	15.2	220.74	59.027	7.0	279.80	66.431	16.6
115.31	16.005	54.7	9.55	1.140	11.8	220.98	59.051	5.3	279.87	66.441	0.6
115.71	16.302	53.4	20.06	2.571	7.1	221.11	59.064	7.1	279.92	66.448	4.4
115.91	16.450	52.8	20.16	2.587	8.3	227.85	59.741	6.5	280.11	66.465	2.9
116.27	16.718	52.8	20.26	2.603	14.7	229.98	59.954	1.4	280.19	66.468	5.2
116.41	16.822	55.4	20.46	2.634	12.6	232.14	60.171	0.9	280.19	66.468	3.5
116.51	16.896	65.4	20.56	2.650	12.8	239.21	60.892	2.4	280.29	66.472	3.5
117.01	17.270	70.1	20.66	2.666	13.2	243.71	61.385	4.7	280.50	66.481	3.5
117.40	17.563	61.4	22.20	2.908	9.3	245.21	61.549	9.7	280.51	66.482	3.2
117.70	17.628	57.1	28.70	3.314	8.2	247.08	61.753	0.2	280.51	66.482	2.5
117.90	17.650	48.9	40.60	3.795	8.6	248.46	61.904	1.7	280.69	66.489	3.3
118.10	17.672	50.4	50.10	4.260	2.5	256.21	62.752	9.4	280.81	66.494	4.7
118.30	17.694	44.4	58.35	4.938	3.9	256.81	62.818	5.9	280.81	66.494	2.9
118.50	17.716	30.5	69.19	5.784	3.5	257.13	62.853	5.3	280.86	66.496	2.9
118.70	17.738	46.7	75.94	6.309	3.1	257.56	62.900	5.3	281.11	66.507	4.7
118.90	17.760	37.3	89.90	7.394	3.6	257.87	62.934	5.2	281.20	66.511	4.1
119.40	17.815	41.5	98.10	8.032	27.6	258.11	62.960	5.4	281.39	66.519	6.7
119.60	17.837	44.2	98.30	8.048	1.7	258.17	62.967	4.0	281.41	66.520	4.8
119.80	17.859	47.1	104.51	10.361	4.0	258.63	63.017	2.9	281.60	66.528	2.3
120.00	17.881	44.2	106.01	10.939	1.4	258.87	63.060	2.7	281.71	66.532	2.1
120.20	17.903	45.3	106.01	10.939	13.9	259.26	63.159	3.3	281.81	66.537	0.6
120.60	17.947	44.3	107.51	11.289	1.6	259.47	63.212	4.9	282.01	66.545	5.5
121.31	19.200	41.8	107.51	11.289	11.4	259.60	63.245	4.6	282.21	66.554	1.6
122.81	22.817	41.7	109.01	11.640	1.5	260.22	63.401	2.5	282.21	66.554	1.9
124.31	22.849	42.1	110.51	11.991	2.1	260.64	63.507	4.5	282.41	66.562	5.0
126.77	22.900	26.8	112.01	12.340	1.9	260.91	63.556	5.5	282.62	66.571	2.2
128.27	22.932	37.4	113.51	25.945	1.5	266.35	64.170	9.8	282.70	66.574	3.5
129.65	22.961	41.2	121.15	36.020	0.1	267.31	64.279	18.8	283.32	66.601	0.5
131.53	23.000	31.4	122.65	36.311	0.2	267.51	64.307	18.3	284.20	66.638	7.8
132.65	23.024	14.2	123.48	36.473	0.6	267.72	64.343	12.6	285.10	66.676	0.1
135.74	23.089	31.6	134.71	41.852	0.2	267.79	64.356	11.2	285.16	66.679	1.6
137.24	23.120	28.6	137.51	45.031	0.6	267.82	64.361	6.2	289.40	66.855	2.5
140.06	23.179	27.7	138.01	45.989	1.0	267.92	64.378	12.5	294.66	67.073	4.2
141.56	23.211	24.2	138.61	47.140	0.4	268.11	64.411	12.2	298.58	67.235	1.0
147.34	23.332	37.6	138.71	47.332	0.3	268.41	64.463	10.6	304.33	67.473	2.6
148.84	23.364	32.1	138.81	47.523	0.8	268.68	64.509	12.5	307.50	67.604	1.2
150.36	23.396	34.1	139.23	47.640	1.0	268.92	64.551	13.0	313.81	67.865	5.7
151.71	23.424	3.5	139.45	47.662	0.6	269.10	64.582	9.5	317.99	68.038	4.4
153.21	23.456	25.0	142.27	48.332	0.4	269.35	64.625	5.7	322.90	68.242	3.8
154.71	23.487	31.6	142.31	48.346	0.7	269.44	64.640	14.1	323.30	68.258	8.4
156.02	23.515	38.8	142.48	48.406	0.9	269.54	64.658	8.2	327.01	68.412	8.1
157.52	23.546	18.6	142.71	48.488	1.4	269.71	64.687	6.4	331.72	68.606	2.2
160.11	23.609	36.0	142.88	48.548	1.2	269.89	64.718	8.7	332.80	68.651	5.9
160.65	23.849	21.0	143.11	48.629	0.7	270.10	64.754	7.5	361.56	69.841	6.6
162.15	24.517	38.3	143.29	48.693	1.1	270.31	64.790	10.0			
163.65	25.185	26.8	143.61	48.805	3.0	270.50	64.823	5.6			
164.51	25.567	22.3	143.77	48.860	2.1	270.71	64.859	7.7			
166.01	26.235	31.3	143.81	48.873	2.5	270.89	64.890	8.0	1.10	0.124	12.3
169.20	27.655	20.6	144.21	49.010	2.8	271.07	64.922	5.0	4.54	0.513	14.0
169.50	27.788	21.0	144.52	49.117	2.5	271.11	64.928	5.7	4.87	0.550	14.8
170.20	28.100	26.1	144.79	49.209	1.7	271.46	64.989	4.8	4.94	0.558	22.5
171.00	28.227	22.7	145.11	49.319	2.8	271.71	65.032	4.4	5.34	0.603	20.9
171.20	28.258										

Appendix B. (Continued).

Sub-bottom Depth (m)	Age (Ma) ^a ^b	Sediment (%)	Sub-bottom Depth (m)	Age (Ma) ^a ^b	Sediment (%)	Sub-bottom Depth (m)	Age (Ma) ^a ^b	Sediment (%)	Sub-bottom Depth (m)	Age (Ma) ^a ^b	Sediment (%)
Site 528 (Cont.)			Site 528 (Cont.)			Site 528 (Cont.)			Site 529 (Cont.)		
9.05	1.022	27.6	19.75	1.907	19.1	198.70	32.496	0.2	129.81	26.185	5.3
9.05	1.022	27.6	19.85	1.922	18.4	207.94	33.668	3.1	136.31	27.678	15.9
9.15	1.033	21.3	19.95	1.937	15.9	225.41	35.784	0.9	136.31	27.678	16.5
9.15	1.033	21.3	20.05	1.952	16.0	225.67	35.820	0.6	137.81	28.022	14.4
9.35	1.056	13.2	20.15	1.966	15.0	227.50	37.051	0.1	137.81	28.022	13.4
9.35	1.056	13.2	20.26	1.982	15.3	227.54	37.063	0.1	139.31	28.409	17.6
9.44	1.066	8.6	20.49	2.016	14.2	236.40	39.688	1.1	139.31	28.409	17.6
9.45	1.067	8.6	20.53	2.022	13.7	236.48	39.711	1.0	142.61	29.288	13.3
9.55	1.078	23.4	20.65	2.040	12.9	237.60	40.043	1.6	142.61	29.288	6.1
9.55	1.078	23.4	20.85	2.069	12.9	237.98	40.156	0.8	144.11	29.688	6.3
9.75	1.101	22.9	22.15	2.261	6.6	246.18	44.794	1.5	144.11	29.688	6.3
9.75	1.101	22.9	22.55	2.320	17.0	246.40	44.920	2.0	145.61	30.087	5.0
9.95	1.124	15.7	22.75	2.349	13.9	247.90	45.776	8.6	145.61	30.087	4.9
9.95	1.124	15.7	22.75	2.349	13.9	249.40	46.439	8.4	147.11	30.487	3.3
10.05	1.135	18.6	22.95	2.379	14.1	250.44	46.784	5.2	148.61	30.886	3.6
10.05	1.135	18.6	23.35	2.437	5.8	250.60	46.837	2.4	150.11	31.286	3.9
10.15	1.146	14.8	23.65	2.482	11.6	252.00	47.302	1.8	150.11	31.286	3.7
10.15	1.146	14.8	23.65	2.482	11.6	255.51	48.338	1.9	154.91	32.565	4.7
10.25	1.158	19.8	23.75	2.496	11.0	255.80	48.415	3.0	156.41	32.964	2.8
10.25	1.158	19.8	23.75	2.496	11.0	256.61	48.632	2.5	156.41	32.964	2.5
10.35	1.169	19.6	24.05	2.540	10.7	257.47	49.311	1.8	160.91	34.163	5.7
10.35	1.169	19.6	24.25	2.570	11.3	258.51	50.507	1.6	170.73	34.774	10.3
10.45	1.180	22.4	24.45	2.599	11.8	258.90	50.747	2.7	175.23	34.870	6.7
10.45	1.180	21.8	24.68	2.633	18.7	260.51	51.741	2.3	176.73	34.901	5.6
10.55	1.191	20.2	28.70	3.123	17.7	263.01	52.630	1.6	176.73	34.901	5.4
10.55	1.191	20.2	32.90	3.237	20.3	266.60	53.388	2.4	182.13	35.016	4.3
10.62	1.199	16.2	34.85	3.290	8.2	269.70	54.018	1.4	183.63	35.048	7.8
10.62	1.199	16.2	35.96	3.320	16.0	275.00	54.503	2.0	185.13	35.080	5.5
10.75	1.214	23.1	36.66	3.339	10.5	284.11	55.337	2.4	186.63	35.173	5.9
10.75	1.214	23.1	37.80	3.370	12.9	284.30	55.354	2.2	188.13	35.370	6.5
10.83	1.223	20.5	42.20	3.489	13.4	285.74	55.438	2.3	190.21	35.643	7.4
10.85	1.225	20.5	43.55	3.525	18.5	294.00	55.775	3.8	191.71	35.840	6.8
10.95	1.237	17.6	43.95	3.536	12.3	306.46	56.284	3.5	193.21	36.037	8.3
10.95	1.237	17.6	44.15	3.542	16.5	313.96	57.650	2.8	194.71	36.234	3.3
10.96	1.238	17.4	44.25	3.544	16.1	314.02	57.653	7.3	195.23	36.302	6.7
11.03	1.246	24.6	44.35	3.547	40.9	322.58	58.212	3.8	197.42	36.589	3.1
11.05	1.248	24.5	44.45	3.550	17.0	333.11	58.898	9.1	198.78	36.767	5.0
11.15	1.259	24.6	44.55	3.553	17.9	334.30	59.027	6.0	198.99	36.795	5.0
11.15	1.259	24.6	44.75	3.558	13.6	350.78	61.124	6.6	199.19	36.821	3.4
11.25	1.270	20.9	45.15	3.569	13.7	361.50	61.448	6.8	199.49	36.861	2.6
11.25	1.270	20.9	45.25	3.572	20.5	361.98	61.463	8.6	200.13	37.059	22.8
11.35	1.282	23.0	45.35	3.574	28.6	370.74	61.728	13.3	200.29	37.133	20.7
11.55	1.304	24.5	45.56	3.580	24.9	379.13	61.983	8.5	200.77	37.357	28.8
11.55	1.304	24.5	46.10	3.595	12.9	380.52	62.075	6.2	201.00	37.465	30.7
11.64	1.314	18.0	48.01	3.703	18.0	383.05	62.307	8.1	201.38	37.642	24.3
11.65	1.316	18.0	51.01	3.884	14.7	383.07	62.309	6.6	201.63	37.759	36.0
11.75	1.327	13.6	55.33	4.394	9.1	390.77	63.016	11.6	202.19	38.020	24.2
11.75	1.327	13.6	57.79	4.609	10.3	391.72	63.160	9.9	202.57	38.197	18.4
11.85	1.338	20.1	61.56	4.797	5.9	393.21	63.905	13.3	202.83	38.318	24.3
11.85	1.338	20.2	64.09	4.922	5.0	398.53	65.292	6.2	203.50	38.631	21.6
11.95	1.349	23.8	65.70	5.005	4.8	400.31	65.587	40.1	203.52	38.640	21.8
12.15	1.372	19.8	66.23	5.055	6.5	401.32	65.691	6.7	204.00	38.864	21.7
12.35	1.395	16.6	70.66	5.471	3.2	403.16	65.880	12.6	205.19	39.420	23.0
12.35	1.395	25.0	77.64	6.128	1.8	404.38	66.006	29.6	205.38	39.508	25.9
12.55	1.417	45.6	81.10	6.454	3.4	407.00	66.460	19.6	206.69	40.120	23.2
12.65	1.429	26.0	87.60	7.065	2.7	407.00	66.460	37.2	207.00	40.264	15.0
12.73	1.438	24.6	93.20	7.592	1.3	407.42	66.479	10.0	207.34	40.423	30.5
13.15	1.470	33.5	98.76	8.115	1.8	408.00	66.504	6.4	208.53	40.978	10.9
13.35	1.483	30.6	99.10	8.147	1.7	424.48	67.318	23.4	250.91	55.282	3.6
13.55	1.497	11.1	100.70	8.298	2.4	428.37	67.520	16.6	262.26	56.132	2.2
13.75	1.510	22.6	105.55	9.437	6.2	438.85	68.065	14.5	287.10	59.367	18.5
13.86	1.517	24.3	106.99	9.937	7.9	453.55	68.828	73.5	295.56	59.591	17.4
13.95	1.523	18.2	108.08	10.315	7.1				298.58	59.671	18.4
14.05	1.529	28.7	111.30	11.122	5.5				300.07	59.711	2.8
14.15	1.536	22.1	111.95	11.263	25.2				305.08	59.844	10.4
14.35	1.549	20.3	112.95	11.480	5.8	7.61	0.999	32.8	306.65	59.885	10.3
14.75	1.575	26.3	113.15	11.524	4.6	79.39	21.204	11.1	308.17	59.926	2.7
14.95	1.588	12.7	113.24	11.543	4.3	88.89	22.950	7.3	314.55	60.095	10.1
15.05	1.595	18.8	116.91	12.534	2.3	95.39	23.092	9.6	315.81	60.184	7.3
15.18	1.603	21.2	118.90	16.514	3.1	96.89	23.125	20.6	324.29	60.908	12.4
15.25	1.608	20.1	119.15	16.523	2.8	99.89	23.191	15.5	325.57	61.025	29.5
15.35	1.615	19.5	122.25	16.637	3.2	101.31	23.222	13.4	325.59	61.026	19.3
15.75	1.641	28.8	128.70	16.872	5.4	102.81	23.255	12.2	328.56	61.296	17.8
15.86	1.648	23.2	132.50	17.333	0.4	109.31	23.397	39.6	335.07	61.675	11.1
15.95	1.654	17.0	143.10	17.932	0.3	112.31	23.463	21.3	338.01	61.745	15.1
16.15	1.667	19.1	157.03	22.094	0.3	115.81	23.540	15.8	341.14	61.820	4.9
19.15	1.864	25.5	166.20	24.336	3.1	117.31	23.573	14.7	352.09	62.408	7.9
19.26	1.871	20.7	177.50	27.061	0.8	120.31	24.004	11.5	360.30	63.396	6.1
19.46	1.884	20.1	185.60	29.464	0.6	121.81	24.348	11.8	362.02	63.603	10.1
19.55	1.890	21.0	195.10	31.950	0.2	125.31	25.152	4.8			
19.65	1.897	20.5				129.80	26.183	9.4			

^a Data from both Cambridge (NJS) and Keil (DF).^b Age estimated by interpolation between control levels for Table I.